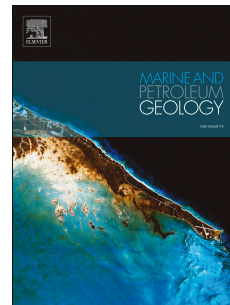


# Accepted Manuscript

Failure to predict igneous rocks encountered during exploration of sedimentary basins: A case study of the Bass Basin, Southeastern Australia

Douglas Watson, Simon Holford, Nick Schofield, Niall Mark



PII: S0264-8172(18)30440-9

DOI: <https://doi.org/10.1016/j.marpetgeo.2018.10.034>

Reference: JMPG 3546

To appear in: *Marine and Petroleum Geology*

Received Date: 21 July 2018

Revised Date: 18 October 2018

Accepted Date: 19 October 2018

Please cite this article as: Watson, D., Holford, S., Schofield, N., Mark, N., Failure to predict igneous rocks encountered during exploration of sedimentary basins: A case study of the Bass Basin, Southeastern Australia, *Marine and Petroleum Geology* (2018), doi: <https://doi.org/10.1016/j.marpetgeo.2018.10.034>.

This is a PDF file of an unedited manuscript that has been accepted for publication. As a service to our customers we are providing this early version of the manuscript. The manuscript will undergo copyediting, typesetting, and review of the resulting proof before it is published in its final form. Please note that during the production process errors may be discovered which could affect the content, and all legal disclaimers that apply to the journal pertain.

1 Failure to predict igneous rocks encountered during exploration of  
2 sedimentary basins: a case study of the Bass Basin, Southeastern  
3 Australia

4 Douglas Watson<sup>a</sup>, Simon Holford<sup>b\*</sup>, Nick Schofield<sup>a</sup>, Niall Mark<sup>a</sup>.

5 <sup>a</sup> *Department of Geology & Petroleum Geology, University of Aberdeen, AB24 3UE, UK*

6 <sup>b</sup> *Australian School of Petroleum, Santos Petroleum Engineering Building, University of  
7 Adelaide, Adelaide, SA 5005, Australia.*

8 \*Corresponding author

9 *E-mail address: [simon.holford@adelaide.edu.au](mailto:simon.holford@adelaide.edu.au) (S. Holford).*

10 **Abstract:** The Bass Basin, a Mesozoic-Cenozoic intra-continental rift basin along the  
11 southern Australian continental shelf, offers an excellent natural laboratory for examining  
12 igneous rocks in the subsurface. Igneous material within the basin is manifested as a mixture  
13 of predominately mafic extrusive and intrusive rocks, mainly Cretaceous-Palaeocene and  
14 Oligo-Miocene in age. Igneous rocks have been encountered in 20 out of 36 (55.6%)  
15 exploration wells drilled within the Bass Basin, but the presence of these has historically been  
16 poorly predicted; of the first 11 exploration wells to penetrate igneous rocks, their presence  
17 was not predicted in pre-drill interpretations. We present a series of case studies from wells  
18 that unexpectedly encountered igneous rocks. The first of these wells (Bass-1) targeted a  
19 carbonate reef structure which instead penetrated the flank of a submarine volcano. In  
20 another notable example (Flinders-1 well), a relatively discontinuous high-amplitude seismic  
21 reflection thought to be a clastic reservoir was found to be an igneous intrusion with a  
22 relatively unusual composition. A number of these incidents, where igneous rocks were  
23 unexpectedly encountered, can be accounted for by human factors, such as a sparsity of  
24 good quality data and a lack of knowledge transfer as companies entered and left basin  
25 during different phases of exploration. However, a number of examples, particularly the  
26 unexpected occurrence of igneous intrusions, appear to have been caused by anomalously  
27 low acoustic impedance contrasts between igneous rocks and surrounding sedimentary  
28 sequences. Our findings have generic implications for other sedimentary basins impacted by  
29 magmatic activity, such as the importance of integrating available outcrop data in the  
30 absence of nearby well control, and the value of fully appraising previous exploration results.

31 *Keywords:*

32 Volcanics  
33 Exploration  
34 Pre-drill prediction  
35 Southern Australia  
36 Bass Basin

37

38

39 **1. Introduction**

40 Igneous rocks are routinely encountered within sedimentary basins undergoing  
41 active hydrocarbon exploration and production, notably including basins on the  
42 North Atlantic continental margin such as the Faroe-Shetland Basin (Rateau et al.  
43 2013; Schofield et al. 2015; Mark et al. 2018; Hardman et al. 2018) and the Vøring and  
44 Møre basins (Planke et al. 2000; 2005; Gernigon et al. 2004; Mjelde et al. 2007;  
45 Hansen et al. 2011; Omosanya et al. 2016, 2017), the South Lokichar Basin of the East  
46 African Rift (Christopherson 2016; Purcell 2017), the Neuquen Basin, Argentina  
47 (Rabbell et al. 2018) and the Santos Basin, Brazil (Ojeda 1982; Chang et al.1992; Fiduk  
48 et al. 2004; Alves et al. 2015). Within the last two decades there has been a plethora  
49 of fieldwork and sub-surface research concerning igneous rocks in sedimentary  
50 basins, such as continental flood basalts (Self et al. 1997; Single & Jerram 2004;  
51 Jerram & Widdowson 2005; Nelson et al. 2009) and igneous intrusion plumbing  
52 systems (Davies et al. 2002; Smallwood & Maresh 2002; Thomson & Schofield 2008;  
53 Jackson et al. 2013; Magee et al. 2015; Schofield et al. 2015; Senger et al. 2017). This  
54 research has revealed a wealth of complex architecture and internal heterogeneity,  
55 for example stacked, anastomosing compound subaerial lava flows, laterally  
56 extensive subaerial tabular lava flows and air-fall tuffs and saucer-shaped igneous  
57 intrusions. For hydrocarbon explorationists, understanding the internal and lateral  
58 heterogeneity of igneous rocks in the subsurface is critical for accurate time-depth  
59 conversion of sub-basalt (Lennon et al. 1999) and intra-basaltic reservoir intervals  
60 (Duncan et al. 2009; Poppitt et al. 2016; Hardman et al. 2018), mapping the lateral

61 continuity of seals (O'Halloran and Johnstone 2001; Schutter 2003 and references  
62 therein; Loizou et al. 2014) and predicting potential drilling issues such as low rates  
63 of penetration through abrasive, crystalline extrusive and intrusive rocks (Archer et al.  
64 2005; Millet et al. 2016; Mark et al. 2018).

65         Within the Bass Basin, located offshore southern Australia between Victoria  
66 and Tasmania, 20 out of 36 (55.6%) of exploration wells drilled to date have  
67 encountered igneous lithologies. These igneous rocks are present within strata above  
68 and below the reservoirs of the producing Yolla gas field in the Bass Basin (Lennon et  
69 al. 1999) whilst Campanian extrusive lava flows form the top seal of the Kipper Field  
70 in the contiguous Gippsland Basin (O'Halloran and Johnstone, 2001), emphasising  
71 the importance of detailed, regional characterisation. There have been several  
72 previous studies of the igneous rocks in the Bass Basin, including investigation of  
73 their geochemical composition and age (Blevin et al. 2003; Meeuws et al. 2016), the  
74 mode of emplacement and seismic expression of the volcanics (Reynolds et al. 2018),  
75 and the impact of the intrusive and extrusive volcanics on the petroleum system  
76 (Holford et al. 2013). Previous work however, has generally overlooked the fact that  
77 explorers have consistently failed to predict the presence of igneous material prior to  
78 drilling in the Bass Basin; of the 20 exploration wells to encounter igneous rocks, on  
79 13 occasions (65%) the igneous rocks were not predicted prior to drilling.

80         This study focuses primarily on the geophysical properties of these igneous  
81 rocks and the surrounding lithologies, which ultimately governs their expression in  
82 seismic reflection data, with lithological calibrations provided by thin-section



83 petrography and whole rock geochemistry. Geological interpretations are  
84 synthesised with well-specific exploration contexts, in order to establish holistic  
85 understandings as to why particular penetrations of igneous material were  
86 unexpected. We propose that the difficulties in predicting these igneous rocks can be  
87 traced back, in part, to their magmatic composition and the nature of the  
88 surrounding host rock. In particular, the acoustic impedance contrast between the  
89 igneous rocks and host rock strata, generally high in sedimentary basins (Planke et al.  
90 2000; Smallwood & Maresh 2002; Schofield et al. 2015; Magee et al. 2015; Mark et al.  
91 2018), appears markedly lower within the Bass Basin. This is due to several  
92 lithological factors, including an abundance of high acoustic impedance coals in the  
93 overburden acting as a seismic transmission filter. A failure to transfer and absorb  
94 knowledge as companies left the basin and new ones entered, also appears to be a  
95 contributing factor to the failure to accurately predict subsurface igneous rocks. Our  
96 findings have wider implications for future exploration within the Bass Basin, and also  
97 for other sedimentary basins impacted by volcanism, including the importance of  
98 integrating outcrop data in the absence of offset well data.

## 99 **2. Regional Geology**

100 The Bass Basin is an intracratonic rift basin that forms part of a failed arm of  
101 the Southern Margin Rift System, located along Southern Australia (Fig. 1a), which  
102 formed as a result of the initial continental break up of Eastern Gondwana as  
103 Australia and Antarctica began to separate (Stagg et al. 1990). Australia's Southern  
104 Margin, including the Bass Basin, underwent multiple phases of Late Mesozoic to

105 Early Cenozoic rifting (Cummings et al. 2004; Blevin & Cathro 2008), punctuated by  
106 periods of post-rift uplift and inversion (Holford et al. 2014). The Bass Basin did not  
107 evolve into a passive-margin basin, in contrast to the contiguous Otway Basin (to the  
108 northwest) and Gippsland Basin (to the northeast), as the locus of rifting moved to  
109 the south of Tasmania (Palmowski et al. 2004; Blevin et al. 2005; Meeuws et al. 2016).

110 The Bass Basin is bounded by major basement structural highs (the King Island  
111 High to the northwest and the Bassian Rise to the east) and is divided into two sub-  
112 basins (Fig. 1a), which are both composed of a series of grabens and half-grabens  
113 characterised by variable amounts and rates of subsidence (Blevin 2003). The Cape  
114 Wickham Sub-basin forms the western portion of the Bass Basin, and is characterised  
115 by normal faults that generally dip, and therefore result in sedimentary packages that  
116 thin, towards the southwest. The Durroon Sub-basin, conversely, contains normal  
117 faults predominantly dipping toward the northeast. The Cape Wickham and Durroon  
118 sub-basins are separated by the Chat Accommodation Zone, an ~NNE-SSW trending  
119 zone of accommodation, likely related to a terrane boundary between Proterozoic  
120 metasediments to the west (Cape Wickham Sub-basin) and Palaeozoic  
121 metasediments and granitic intrusions to the east (Durroon Sub-basin) (Blevin et al.  
122 2003).

123 The sedimentary succession of the Bass Basin ranges from Early Cretaceous to  
124 Recent in age (Lennon et al. 1999) (Fig. 2). Several stratigraphic nomenclatures have  
125 been used, with this study adopting the lithostratigraphic framework of Lennon et al.  
126 (1999) and Cummings et al. (2002); the megasequences (tectonically controlled

127 cycles) defined by Blevin (2003) & Cummings et al. (2004) are also shown for  
128 reference (Fig. 2). From the Cretaceous to early Eocene, sedimentation was  
129 predominantly lacustrine to fluvial-deltaic, represented by the Eastern View Coal  
130 Measures (EVCM) Group. From the Mid-Eocene onwards, marine conditions prevailed  
131 with initial deposition of shallow marine mudstones (Demon's Bluff Formation), then  
132 later open marine calcareous siltstones, marls and carbonates (Torquay Group)  
133 (Lennon et al. 1999; Blevin et al. 2003).

#### 134 2.1. Magmatic & volcanic history of the Bass Basin

135 The magmatic and volcanic history of the Bass Basin is broadly divided into  
136 four phases (Meeuws et al. 2016). The earliest evidence for volcanism recognised is  
137 the apparent presence of *Early Cretaceous* volcanoclastic sediments within the Otway  
138 Group, possibly sourced from the northwest from basaltic volcanism near the  
139 Hawkesdale area of Western Victoria (Duddy 2003). *Mid-Cretaceous* syn-rift  
140 weathered amygdaloidal basalts, interbedded with Aptian aged sediments, are  
141 encountered in the Durroon Sub-basin (within the Durroon-1 well), with a possible  
142 origin related to the onset of rifting in the Tasman Basin (Blevin 2003; Meeuws et al.  
143 2016). The extent of these volcanics is unclear, particularly within the Cape Wickham  
144 Sub-basin, due to a lack of well penetrations of Middle Cretaceous strata (Blevin  
145 2003; Meeuws et al. 2016). A *Late Cretaceous-Palaeocene* syn-rift volcanic event,  
146 manifested as lava flows, is more widely recognised, for instance in the Yolla and  
147 Dondu troughs of the Cape Wickham Sub-basin, and in the Bark Trough of the  
148 Durroon Sub-basin (Meeuws et al. 2016). The age of these lava flows is determined

149 through dating of the palynoflora of the interbedded sediments (Baillie 1993). Finally  
150 a basin-wide *Oligocene-Miocene* post-rift magmatic episode is represented by a  
151 series of submarine monogenetic volcanoes and associated feeder intrusions  
152 (Meeuws et al. 2016; Holford et al. 2017; Reynolds et al. 2018).

153

## 154 2.2. *Exploration History and Petroleum System Elements of the Bass Basin*

155 Hydrocarbon exploration has been ongoing in the Bass Basin since the 1960s and  
156 has occurred in distinct cycles (Blevin 2003). In total 45 wells have been drilled, 36 of  
157 which are exploration wells (Fig. 1b). The Bass Basin hosts a working, terrestrial-based  
158 petroleum system (Blevin 2003) with Palaeocene to Early Eocene EVCM coals forming  
159 the dominant source rock (Boreham et al., 2003), and is prospective for both oil and  
160 gas (Blevin 2003). Proven reservoirs are mainly present within Palaeocene and lower  
161 Eocene fluvial-deltaic sandstones of the EVCM (Boreham et al., 2003). The Demon's  
162 Bluff Fm. forms the regional seal (Lennon et al. 1999; Blevin 2003). Hydrocarbon  
163 shows have been identified in a number of wells, though hydrocarbon accumulations  
164 are observed only in the Pelican, Rockhopper, Trefoil, White Ibis, Bass and Yolla  
165 structures. These discoveries are mainly gas with minor oil accumulations (Blevin  
166 2003). Presently, Yolla (gas and gas condensate) is the only producing field.

167

168

## 169 3. **Data and methodology**

### 170 3.1. Data

171 The main dataset used in this study is the publicly released commercial hydrocarbon  
172 well data from the Bass Basin (Fig. 1b). From these wells a range of datasets were  
173 examined and synthesised, including; wireline data (e.g. gamma ray, resistivity,  
174 neutron porosity etc.), composite well logs, geological end of well reports, and core  
175 and ditch cuttings. Seismic datasets were also examined, including regional 2D lines  
176 and the Shearwater Marine and Yolla 3D seismic surveys (Fig. 1b) to characterise  
177 seismically identifiable volcanic units, and to understand the basin architecture.

### 178 3.2. Subsurface Identification and classification of igneous rocks

#### 179 3.2.1. Micro-scale (<0.5 m): core and ditch cuttings

180 Within the Bass Basin a variety of igneous rocks are present throughout the  
181 stratigraphy, which can be recognised at a number of different scales. We define  
182 micro-scale as any dataset at hand-specimen scale. Figure 3 summarises the main  
183 micro-scale datasets and workflow utilised in this study, with each source of  
184 information detailed further below.

185 Ditch cuttings, the rock fragments brought to the rig site via the drilling fluid,  
186 provide a ubiquitous source of information with regards to the igneous rocks  
187 encountered in the Bass Basin. Core is rarely obtained through the igneous rocks of  
188 the Bass Basin, though side-wall cores are more commonly acquired. Thin-sections  
189 from side-wall cores are critical to elucidating the grain-size and mineralogy, both of  
190 which are key to determining magmatic mode types. Thin-section micrographs, and

191 associated mineralogy descriptions, were collated from geological end of well  
192 reports, and from an unpublished study commissioned by Geoscience Australia.

193 Mineralogical descriptions are supported by geochemical data, and this study  
194 in particular utilised x-ray fluorescence (XRF) analysis carried out by Geoscience  
195 Australia (GA) on a number of igneous rock samples (including ditch cuttings and  
196 core) from the Bass Basin. Plotting the major oxides (on a Total Alkali Silica diagram,  
197 e.g. Le Bas et al. 1986) and trace elements (on a Winchester & Floyd, 1977,  
198 discrimination diagram) allows determination of the magma type, which in turn  
199 influences the well log character (detailed in the succeeding "*Meso-scale: geophysical*  
200 *logs*" sub-section of this paper).

201 Thermal maturity data, such as spore colour index and vitrinite reflectance,  
202 provide further micro-scale information for characterising subsurface igneous rocks,  
203 particularly in demonstrating zones of elevated palaeotemperature. The significance  
204 of elevated palaeotemperature is underpinned by a number of studies that  
205 document the negligible thermal impact of extrusive lava flows (e.g. Archer et al.  
206 2005; Grove 2014; Schofield et al. 2015) relative to igneous intrusions (Jolley & Bell  
207 2002; Archer et al. 2005; Holford et al. 2013). Ultimately, evidence of elevated  
208 palaeotemperature above and below a particular igneous unit can help distinguish it  
209 as intrusive in origin.

210 *Meso-scale (>0.5 m): geophysical logs*

211 Geophysical logs, such as gamma ray, electrical resistivity and sonic velocity, offer a  
212 useful dataset for examining the igneous rocks in the Bass Basin at a scale  $>0.5$  m  
213 (the vertical resolution of common downhole tools c.f. typical sampling rates of  
214  $\sim 0.15$  m). Igneous rocks exhibit a wide variety of log motifs, which are largely  
215 controlled by mineralogy (summarised in Fig. 4). Mafic igneous rocks, such as basalt,  
216 represent the most common type of igneous rock in the Bass Basin (Meeuws et al.  
217 2016) and these typically exhibit low gamma values (10-40 API) (Fig. 4a). This reflects  
218 the abundance of minerals such as pyroxene and plagioclase which contain little  
219 potassium, thorium and uranium (Serra et al. 1980; Planke 1994; Bartetzko et al.  
220 2005). Silicic igneous rocks, in contrast, typically measure higher gamma values (40-  
221 100 API) (Fig. 4b) due to the presence of minerals such as potassium feldspar (Serra  
222 et al. 1980; Delpino & Bermudez 2009; Mark et al. 2018). Igneous rocks can also be  
223 divided into crystalline and volcanoclastic units (clastic rocks containing a high  
224 proportion of volcanic derived material) (Mathisen & McPherson, 1991). Crystalline  
225 igneous rocks, such as compound lavas (Fig. 4c), tabular lavas (Fig. 4d) and igneous  
226 intrusions (Fig. 4e) typically display high resistivity (2-300 Ohm m) and low neutron  
227 porosity values (0.08-2%), reflecting their typically low primary porosity (Planke 1994;  
228 Bartetzko et al. 2005; Millet et al. 2015 ; Watson et al. 2017; Mark et al. 2018).  
229 Volcanoclastic rocks, which includes tuffaceous rocks (lithified ash) (Fig. 4f),  
230 hyaloclastites (Fig. 4g) and intra-lava claystones (Fig. 4g), demonstrate lower  
231 resistivity (2-20 Ohm m) and higher neutron porosity values ( $\sim 45$ -30%) due to the

232 presence of clay-bound water (Planke 1994; Bartetzko et al. 2005; Watton et al. 2014;  
233 Watson et al. 2017).

### 234 3.2.2. Macro-scale (>30 m): Seismic Data

235 Igneous rocks within the Bass Basin can be also investigated at a macro scale i.e. rock  
236 units that are sufficiently thick as to be visible in seismic reflection datasets. Within  
237 the Bass Basin mafic igneous rocks such as basalts and dolerites predominate, which  
238 are typically characterised by high densities (>2.7 g/cc) and fast sonic velocities  
239 (>4000 m/s; >80 ms ft<sup>-1</sup>). There is generally a significant acoustic impedance contrast  
240 between mafic igneous material and the surrounding, lower density sediments  
241 (Smallwood & Maresh 2002; Holford et al. 2012; Magee et al. 2015; Schofield et al.  
242 2015; Eide et al. 2017; Mark et al. 2018). Some previous studies have investigated  
243 volcanic architectures in the Bass Basin using seismic reflection data, particularly vent  
244 complexes and associated feeder intrusions (Reynolds et al. 2018). The seismic  
245 datasets examined in this study are displayed in time with a standard polarity (Sheriff  
246 & Geldart 1995), by which a downwards increase in acoustic impedance corresponds  
247 to a positive amplitude (a hard kick), displayed in red, while a downwards decrease in  
248 acoustic impedance is represented by a negative amplitude (soft kick) displayed in  
249 blue (Fig. 5). Three broad sets of igneous rocks are recognised in seismic (Fig. 5) and  
250 in wells throughout the Bass Basin, as described in detail in Section 4 of this paper.  
251 The igneous rocks within the Bass Basin are broadly present within two major  
252 lithostratigraphic sections: (1) the Torquay Group (Oligocene) and (2) the Eastern



253 View Coal Measures (EVCN) (Late Cretaceous to Early Eocene). The igneous rocks  
254 within the Torquay Group have velocities  $\sim 3000 \text{ m s}^{-1}$ , with a dominant frequency in  
255 the seismic surveys examined between 39-45 Hz (Reynolds et al. 2018). This yields a  
256 vertical seismic resolution between 17-19 m and a vertical detectability of 8-10 m for  
257 igneous units within the Torquay Group, based on  $\lambda/4$  (resolution) and  $\lambda/8$   
258 (detectability) (Widess 1973; Simm & Bacon 2014). For igneous rocks within the  
259 EVCN velocities range from 5000-6600  $\text{m s}^{-1}$ , with a dominant frequency between  
260 29-40 Hz. The seismic resolution of igneous material present within the EVCN is  
261 therefore estimated at approximately 41-43 m, with a vertical detectability between  
262 21-22 m.

263

#### 264 **4. Igneous rock varieties within the Bass Basin**

265 In order to investigate why igneous units have historically been poorly predicted in  
266 the Bass Basin, the character of the different igneous lithologies present needs to be  
267 established. In this section we detail the well log character of the igneous rocks  
268 encountered within the Bass Basin, which can be broadly divided into three different  
269 sets based on their mode of emplacement: (1) submarine volcanic rocks (2) igneous  
270 intrusions and (3) subaerial volcanic material. These different types of igneous  
271 lithologies are each characterised by a unique well log character (Fig. 6) and exhibit  
272 variable geographic and stratigraphic distribution across the basin (Fig. 7).

273 4.1. Submarine volcanism products- hyaloclastites and volcanoclastic rocks

274 The shallowest and most widespread of the main sets of igneous rocks recognised  
275 within the Bass Basin is represented by a series of seismically imaged volcanic vents,  
276 between 0.3-1.2 km in diameter (Reynolds et al. 2018) within the Torquay Group.  
277 These vents are interpreted to be submarine volcanoes due to the presence of  
278 underlying feeder intrusions, downlapping reflections within the vents that are typical  
279 of extrusive volcanism, and the fact that the vents sit within a succession of marine  
280 sedimentary rocks (Reynolds et al. 2018). These submarine volcanoes are present  
281 throughout the Bass Basin, and several wells have penetrated the flanks of the  
282 structures, including Bass-1 (Cormorant Trough), Tilana-1 (Dondu Trough), Yolla-1  
283 and Trefoil-1 (Yolla Trough). Core was acquired through the volcanic section within  
284 the Bass-1 well, and in hand-specimens the recovery material consists of a clast  
285 supported conglomerate of dark grey micro-vesicular basalt (Fig. 8) with infilled  
286 calcite. A degree of reworking of the primary volcanic material is indicated by  
287 rounded clasts (Fig. 8b) and normally graded beds 0.2-3 cm in thickness (Fig. 8d).  
288 There are also pyroclastic components within this material, with several sub-angular  
289 vesicular pumice clasts recognised (Fig. 8c).

290 In general, limited wireline log data has been acquired through these  
291 submarine volcanic rocks due to the fact they are hosted within the Torquay Group,  
292 which represents uneconomic overburden within the Bass Basin. The Tilana-1 well,  
293 within the Dondu Trough, contains amongst the best suite of wireline logs acquired  
294 through the volcanics (upper section of Fig. 6). The log motif is characterised by a  
295 generally low, blocky gamma (11-22 API) (Fig. 6a) and moderately high, serrated

296 resistivity (2-15 Ohm m) (Fig. 6b) typical of relatively heterogeneous hyaloclastite  
297 (e.g. McLean et al. 2017). Sonic velocity is moderately fast with a serrated profile (with  
298 an average value of  $97 \text{ ms ft}^{-1}$ ) (fig. 6d). Density and neutron logs have not been  
299 acquired through any of the submarine volcanics packages throughout the Bass  
300 Basin, though a sonic velocity-derived density can be calculated (Fig. 6c) (using the  
301 method of Bartetzko et al. 2005). This gives values generally ranging from 2.15-2.55 g  
302  $\text{cm}^{-3}$ , with lower density zones ( $<1.95 \text{ g cm}^{-3}$ ) possibly representing less compacted  
303 volcanoclastic (e.g. tuffaceous) material.

304 A volcanic edifice was also drilled by the Tasmanian Devil-1 well, located in the  
305 southwest of the Bass Basin, though the well penetrated the crest of the structure, in  
306 contrast to the Yolla-1, Bass-1 and Tilana-1 wells which intersect the flanks of  
307 submarine volcanoes. The volcanic rocks in Tasmanian Devil-1 exhibit high resistivity  
308 (5-2000 Ohm m) and densities ( $2.75\text{-}2.85 \text{ g cm}^{-3}$ ) and fast sonic velocity ( $72\text{-}50 \text{ ms ft}^{-1}$ )  
309 typical of crystalline material, which is mirrored in thin-section by fine grained  
310 crystalline basaltic material. A prominent gradual decrease in gamma ray and  
311 resistivity upwards within the Tasmanian Devil-1 volcanic succession is similar in log  
312 profile to pillow lavas described by Bartetzko et al. (2005). We therefore interpret the  
313 volcanic rocks intersected in Tasmanian-Devil-1 as pillow lavas, representing the up-  
314 dip equivalent of the reworked hyaloclastite and volcanoclastic material encountered  
315 in Bass-1, Yolla-1 and Tilana-1. Such a lateral facies variation also corroborates with  
316 observed lateral seismic amplitude changes within the Yolla submarine volcano  
317 previously attributed to facies changes (Faustmann 1995).

#### 318 4.2. Intrusive magmatic products- igneous intrusions

319 Intrusive igneous rocks are predominantly hosted within the Middle EVCM (Tilana  
320 and Narimba sequences) and have been penetrated in 14 exploration and appraisal  
321 wells (see Fig. 7 for examples). A 64m thick intrusion intersected within Flinders-1,  
322 located along the southern flank of the Pelican Trough, captures much of the  
323 principal features of the igneous intrusions encountered throughout the Bass Basin  
324 (middle section of Fig. 6). The Flinders-1 intrusion log motif is manifested by  
325 relatively low gamma (15-20 API) (Fig. 6e), with high resistivity (17-92 Ohm m) (Fig.  
326 6f), density (2.75-2.84 g cm<sup>-3</sup>) (Fig. 6g) and fast sonic velocity values (58-52 ms ft<sup>-1</sup>)  
327 (Fig. 6h) typical of mafic intrusions (e.g. dolerite). In the upper third section of the  
328 intrusion, however, there is a notable zone of higher gamma (48-74 API) (Fig. 6i) and  
329 marginally lower density (2.62-2.72 g cm<sup>-3</sup>) and slower sonic velocity (69-62 ms ft<sup>-1</sup>).  
330 This high-gamma log character, specifically positioned in the upper third of the  
331 intrusion, is also observed in the Koorkah Terrace (Seal-1) and Cormorant Trough  
332 (Toolka-1A) (Fig. 9). XRF geochemistry from the Seal-1 well depicts two different  
333 magmatic compositions (Fig. 9); the lower gamma material plots as basaltic in  
334 composition, whereas the higher gamma material plots as tephra-phonolite in  
335 composition.

#### 336 4.3. Subaerial volcanism products- lava flows and interbedded 337 volcaniclastic rocks

338 The third broad set of igneous rocks recognised within the Bass Basin is represented  
339 by subaerial volcanic material, such as extrusive lava flows and associated  
340 volcaniclastic units which are interdigitated with terrestrial EVCM sedimentary rocks

341 (e.g. coals and fluvial sandstones, predominantly within the Middle EVCM). These  
342 extrusive lavas are penetrated in 6 structures throughout the basin (Aroo-1/  
343 Rockhopper-1, Trefoil-1, Chat-1, the greater Yolla Field, Tilana-1, Duroon-1; see Fig. 7  
344 for examples). A number of these subaerial lava successions are characterised by  
345 poor wellbore conditions (e.g. hole washout), and therefore geophysical log quality is  
346 generally poor. The Trefoil-1 well, however, contains a diverse suite of good quality  
347 log data (lower section of Fig. 6). Between 3389.6-3460 m there are several units  
348 exhibiting low gamma (18-35 API) (Fig. 6j), high resistivity (20-1800 Ohm m) (Fig. 6k)  
349 and high density values ( $2.6-2.82 \text{ g cm}^{-3}$ ) (Fig. 6l) characteristic of tabular classic lava  
350 flows. A zone of compound lavas (between 3412-3419 m MD) is recognised by  
351 marginally lower density and resistivity (compared to tabular lavas) and a "double  
352 peak" in sonic velocity (Fig. 6m) (e.g. Nelson et al. 2009). Decreases in density and  
353 resistivity distinguish intra-basaltic sandstones from the surrounding low gamma  
354 lavas. Underlying this, from 3460-3524 m (MD,) a package of interbedded shales and  
355 sands, and minor volcanoclastic claystone units are present. Within the Cape Wickham  
356 Sub-basin these terrestrial extrusive lava flows range in age from Late Cretaceous (*T*  
357 *lilliel* pollen zone, Campanian-Maastrichtian) (Trefoil-1 & Yolla-1) to Maastrichtian-  
358 Danian (Tilana-1). Within the Duroon Sub-basin an older Cenomanian subaerial  
359 extrusive lava succession is present (Duroon-1) (Fig. 7).

360

## 361 **5. Case studies of wells where igneous rocks were not predicted prior to** 362 **drilling**

363 44 wells in total have been drilled within the Bass Basin, 36 of which are designated  
364 as exploration wells. These 36 exploration wells are used as the basis for a statistical  
365 review of pre-drill prediction of igneous rocks in the study area; further detail on  
366 these wells is included as Supplementary Material. Appraisal and development wells  
367 (e.g. Yolla-2 to 6) are not included as part of the statistical review as the presence or  
368 absence of igneous rocks would have been already established by the prior  
369 exploration well. Pre-drill lithological predictions versus post-drill actual lithologies  
370 encountered were found in publically released Geological End of Well Report for the  
371 respective wells, sourced from the Australian National Offshore Petroleum  
372 Information Management System (NOPIMS); see Figures 12 and 13 for specific  
373 examples of a pre-drill versus post-drill lithology column. In instances of wells where  
374 igneous rocks were encountered though not predicted pre-drill, we also noted  
375 whether the operator was new to the basin, i.e. whether the well was the first drilled  
376 by the operator or part of their first drilling campaign. The following results have  
377 been established from the wells within the Bass Basin:

- 378 • 20 out of 36 exploration wells encountered igneous rocks (55.6%)
- 379 • In 13 of those 20 exploration wells the igneous rocks encountered were not  
380 predicted pre-drill (65%)
- 381 • Of the 13 wells where igneous rocks were unexpectedly drilled, on 7 occasions  
382 the well was operated by a company new to the basin (53.8%).

383 During the various cycles of exploration within the Bass Basin the incidence of  
 384 igneous rocks not being predicted prior to drilling is consistently high (ranging from  
 385 40-87.5% of exploration wells in a given cycle; Table 1). Of the 13 exploration wells  
 386 that failed to predict the presence of igneous rocks prior to drilling, the following  
 387 section focuses on four noteworthy examples where the pre-drill reservoir target  
 388 instead was found to be high seismic amplitude igneous rocks (Trigg et al. 2003;  
 389 Meeuws et al. 2016).

390 **Table 1:** Statistical breakdown of the number of wells to encounter igneous rocks within the  
 391 Bass Basin, and the proportion of those wells where the presence of those igneous rocks was  
 392 not predicted pre-drill.

Time Period	Total Number of Bass Basin Exploration wells	Number of exploration wells that encountered igneous rocks	Proportion of exploration wells where igneous rocks were not predicted
1965-1974	17	8 (47.1%)	7 (87.5%)
1979-1986	7	5 (71.4%)	2 (40%)
1992-1999	6	3 (50%)	2 (66.7%)
2004-present	6	4 (66.7%)	2 (50%)

393

394

395 *5.1. Bass-1 (1965): Pre drill- Carbonate reef/Post drill- Submarine volcano*

396 Bass-1 was drilled in the Cormorant Trough in 1965 by Esso Australia, and was the  
 397 first well drilled in the Bass Basin. The purpose of the well was to gain stratigraphic  
 398 information from the Cenozoic and Upper Mesozoic sedimentary succession, and to  
 399 test the petroleum potential of a postulated Miocene carbonate reef build up (Fig.  
 400 11) (Blevin et al. 2005). The pre-drill interpretation of carbonates was based on  
 401 presence of Miocene limestones in the adjacent Gippsland Basin (stratigraphic  
 402 equivalent of the Torquay Group (Lennon et al. 1999)), where the nearest offset wells

403 were located. Instead of Miocene carbonates however, ~130 m of interbedded  
404 volcanoclastic rock was intersected instead (Fig. 11). No hydrocarbon shows were  
405 recorded within the volcanoclastic rocks, or indeed the entire drilled succession.

406           5.2.   *Aroo-1 (1974): Pre drill- Stacked fluvial deltaic sandstones/Post drill-*  
407                   *extrusive lava flows*

408 Aroo-1 is located on the north flank of the Yolla Trough, and was drilled by Hematite  
409 Petroleum in 1974. The primary target of Aroo-1 was an amplitude anomaly at the  
410 top of an intra-basin fault block (Fig. 12) (Blevin & Cathro 2008). The amplitude  
411 anomaly was interpreted to be hydrocarbon-bearing sandstones, likely between the  
412 *M. diversus* and *L. balmei* zones within the Middle EVCM (Fig. 12, *predicted*), which are  
413 hydrocarbon bearing within the Pelican Field (Trigg et al. 2003). Upon drilling (Fig. 12,  
414 *actual*) the amplitude anomaly was discovered to be related to a series of stacked  
415 subaerial lava flows and volcanoclastics, and thin (<1m) siltstone and sandstone beds.  
416 In total over 500 m of volcanics and interbedded non-volcanic sedimentary rocks  
417 were encountered before the well terminated 270 m early at 3692 m MD, without  
418 having drilled through the base of the volcanic pile (Fig. 12). Despite the pre-drill  
419 misdiagnosis of the lithological character of the amplitude anomaly, sub-economic  
420 gas condensate shows were logged within sandstones interbedded with the extrusive  
421 volcanics (Trigg et al. 2003). On 3D seismic (from the Shearwater Marine survey) the  
422 top of the extrusive lavas corresponds to a bright hard kick (the pre-drill target) (Fig.  
423 12). The volcanic pile is relatively laterally discontinuous, with the underlying strata  
424 becoming clearer as the volcanics pinch out to the southwest. A climbing reflection



425 beneath the extrusive volcanics (~2.7 sec TWT) exhibits a strata discordant character,  
426 and therefore may represent the underlying intrusive plumbing system of the  
427 subaerial lava flows penetrated in Aroo-1.

428           5.3. *Tasmanian Devil-1 (1984): Pre-drill- EVCM Horst block/Post-drill-*  
429           *Extrusive lava flows*

430 Tasmanian Devil-1 is located over a horst block 20 km south of the Pelican Trough,  
431 and was drilled in 1984 by Weaver Oil & Gas Corporation Australia. In 1984 the  
432 nearest offset well was Pippipa-1, 53 km to the northwest. The purpose of Tasmanian  
433 Devil-1 was to test the hydrocarbon potential of the lower section of the EVCM  
434 (below *M. diversus*) within an interpreted horst block on the flank of a broad graben  
435 structure (Fig. 13a). A bright seismic amplitude reflection overlying the crest of the  
436 structure was interpreted pre-drill as a near-top EVCM sandstone reservoir.

437           The drilled succession matched the pre-drill prognosis until the base of the  
438 Torquay Gp., markedly differing thereafter (Fig. 13b/c). Instead of the Demon's Bluff  
439 Formation and EVCM being encountered (Fig. 13b), Tasmanian the drilled section  
440 passed from Torquay Group siltstones to Cenozoic extrusive lava flows (Fig. 13c). The  
441 bright reflection that was interpreted prior to drilling as marking the top EVCM  
442 instead corresponded to the top of the volcanic pile. After 120 m of basaltic rock was  
443 penetrated the decision was taken to terminate the well prematurely (~959 m MD),  
444 around 130 m shallower than planned termination at 1089 m.

445

446           5.4. *Flinders-1 (1992): Pre-drill- Middle EVCM amplitude anomaly/Post-drill-*  
447           *Igneous intrusion*

448 Flinders-1 was drilled in 1992 by SAGASCO Resources along the southwestern flank  
449 of the Pelican trough. The well was designed to test an amplitude anomaly within a  
450 fault-bounded 3-way closure along a structural trend up-dip of the Pelican Field (Fig.  
451 14). A major part of the rationale behind the Flinders prospect was that hydrocarbon  
452 shows (in the form of fluorescence and elevated gas readings) were encountered by  
453 the Pipipa-1 well drilled 10 years earlier in 1982, located 2 km to the northeast of the  
454 proposed Flinders-1 well (Fig. 14). The shows in Pipipa-1 were encountered within  
455 good reservoir quality sandstones (19-31% porosity, 53-630 md) within the Upper  
456 EVCM. However, the gas volumes in Pipipa-1 were sub-economic and the well was  
457 terminated within the Upper EVCM. The primary objective of Flinders-1 was  
458 interpreted as fluvial sandstones of the lower *M. Diversus* to middle *M. diversus* within  
459 the Middle EVCM, which is at a deeper stratigraphic level than gas encountered  
460 within the Upper EVCM in Pipipa-1.

461 Upon drilling of Flinders-1, the amplitude anomaly proved to be a 70 m thick  
462 dolerite intrusion, and all sandstone units within the well were water bearing.  
463 Modelling the synthetic seismic response (Fig. 14) through the EVCM confirms that  
464 the amplitude anomaly corresponds to a seismically resolvable hard kick created by  
465 the acoustic impedance contrast between the igneous intrusion and the surrounding  
466 EVCM sedimentary rocks (coals, siltstones and sandstones). Post drill evaluation of  
467 both wells reveals that the source rocks within Pipipa-1 are immature, and therefore  
468 the gas shows logged were likely a product of the localised heating of coals by the

469 intrusion encountered in Flinders-1 (Trigg et al. 2003). Had Pipipa-1 drilled 147 m  
470 deeper, it would likely have encountered the Flinders-1 intrusion.

## 471 **6. Discussion**

472 *6.1. Why have igneous rocks within the Bass Basin been so poorly predicted?*

473 *6.1.1. Data quality and availability*

474 In each case study discussed in the previous section of this paper, the wells  
475 were drilled based on sparse 2D seismic reflection data. The quality of the seismic  
476 data these wells were drilled on clearly would have been of a lower quality than the  
477 modern 2D and 3D seismic displayed in this study (Fig. 15). Furthermore, in a number  
478 of instances where the presence of igneous rocks was not predicted prior to drilling a  
479 lack of reliable well control appears to be a common factor. With regards to the  
480 Bass-1 well, the nearest offset wells were located in the Gippsland Basin, 200 km to  
481 the northeast. Consultation of these Gippsland Basin wells would have favoured a  
482 carbonate reef genesis, as opposed to an extrusive volcanic origin (Fig. 11), given the  
483 occurrence of limestone within the Miocene of the Gippsland Basin. In terms of the  
484 Tasmanian Devil-1 well, however, Cenozoic basaltic lavas outcrop ~50 km away in  
485 northwest Tasmania (Meeuws et al. 2016). This outcrop is broadly equidistant with  
486 the nearest offset well at the time (Pipipa-1, located 53 km away to the northwest of  
487 Tasmanian Devil-1) (Fig. 1). A pre-drill seismic interpretation is not included within  
488 the Tasmanian Devil-1 end of well report, though based on the predicted lithologies,  
489 one can be broadly reconstructed (Fig. 13b). In modern seismic data (Fig. 13) a  
490 number of igneous intrusions are clearly identifiable close to the Tasmanian Devil  
491 horst, including a dyke propagating along the north-eastern bounding fault and a

492 saucer-shaped intrusion present to the southwest of the horst. While it is unclear  
493 how the available seismic data prior to drilling was interpreted by explorationists,  
494 consideration of the proximal volcanic rocks onshore Tasmania, and in-turn the  
495 recognition of igneous intrusions off the structure may have changed the  
496 stratigraphic prediction and therefore altered pre-drill risking of the prospect.

497

#### 498 *6.1.2. Cyclical nature of exploration and knowledge sharing*

499 A notable feature of exploration within the Bass Basin is that it has been focused in  
500 distinct cycles through time (exploration timeline depicted in Fig. 10). There is a clear  
501 trend of companies drilling a series of wells, then leaving the basin (often after sub-  
502 economic discoveries), followed later by a new company entering the basin and the  
503 cycle starting anew. In terms of the wells where igneous rocks were encountered but  
504 not predicted prior to drilling in the context of these cycles (visually depicted in Fig.  
505 10), the majority (7/13 wells, 53.8%) were operated by companies that were new to  
506 the basin (i.e. part of their first drilling campaign). Therefore, an important aspect of  
507 the failure to predict igneous rocks pre-drill is arguably the lack of knowledge  
508 transfer between companies leaving and entering the basin. Equally, knowledge  
509 sharing appears not to have effectively taken place between different basins across  
510 Southern Australia. For example, the Sailfish-1 well, drilled in the contiguous  
511 Gippsland Basin in 1971 by NWS Oil & Gas, had a remarkably similar Carbonate reef  
512 pre-drill interpretation to the Bass-1 prospect. Sailfish-1 ultimately drilled a

513 submarine volcano instead of a postulated carbonate reef, precisely as the Bass-1  
514 well had done 6 years earlier in the Bass Basin.

515 *6.1.3. Anomalously low acoustic impedance rocks*

516 A number of the igneous units that were unexpectedly encountered in the Bass Basin  
517 are nevertheless clearly identifiable in modern seismic datasets, particularly the  
518 submarine volcanoes present within the Torquay Group. The only instances where  
519 these submarine volcanoes were not predicted pre-drill appear to be Bass-1 and  
520 Tasmanian Devil-1, where, as discussed earlier, there was limited prior well control.  
521 All the other instances of unexpectedly encountered igneous rocks within the Bass  
522 Basin are either igneous intrusions or terrestrial extrusive lava flows.

523 In terms of understanding why igneous intrusions within the Bass Basin have  
524 been poorly predicted, an instructive comparison can be made with intrusions of a  
525 broadly similar geometry and composition within the Faroe–Shetland Basin  
526 (Northwest European Atlantic continental margin). Specifically, the modelled  
527 synthetic seismic response of the Flinders-1 intrusion can be compared with an  
528 intrusion examined by Mark et al. (2018) (Fig. 16). The intrusion from the Faroe-  
529 Shetland Basin is 47 m thick, hosted within relatively homogenous marine claystone,  
530 and appears as a bright, seismically resolvable hard kick. The Flinders-1 intrusion is  
531 64 m thick, hosted within heterogeneous non-marine sediments, and also images as  
532 a seismically resolvable hard kick. However, despite the fact that the Flinders-1  
533 intrusion is ~1.1 km shallower and present within a higher frequency domain than

534 the Faroe-Shetland Basin intrusion, it appears significantly dimmer. There appear to  
535 be three key contrasting features between the two examples which can help explain  
536 observed differences in acoustic impedance. Firstly, the Flinders-1 intrusion has the  
537 notable occurrence of a raft of less dense silicic intrusive material, which is also  
538 observed in other intrusions within the Bass Basin, which may also account for the  
539 slightly undulating profile of the modelled peak seismic wavelet. The Faroe-Shetland  
540 Basin intrusion in contrast is characterised by uniformly high density dolerite.  
541 Secondly, the relatively homogenous claystone host rock surrounding the Faroe-  
542 Shetland Basin intrusion is likely more favourable for generating high acoustic  
543 impedance, in comparison to the highly interbedded non-marine strata (e.g.  
544 sandstone, siltstone and coal) which hosts the Flinders-1 intrusion. A final important  
545 feature to note is the presence and abundance of coals within the Upper EVC in the  
546 strata above the Flinders-1 intrusion. These coals do not affect the modelled  
547 synthetic seismic response, through their high impedance nature (a high reflection  
548 coefficient) means they likely act as a transmission filter due to large amounts of  
549 seismic energy being reflected as opposed to being transmitted (low transmission  
550 coefficient) (Coulombe & Bird 1996). Ultimately, the coals within the Bass Basin are  
551 known to mask imaging of the strata below, including any intrusions or lava flows  
552 (Blevin 2003).

553 Finally, in terms of the subaerial volcanic rocks (e.g. lava flows) within the Bass  
554 Basin informative comparisons can be made with the top of the extrusive lava pile  
555 within the Faroe-Shetland Basin. The extrusive lavas within the Faroe-Shetland Basin

556 constitute Palaeocene-Eocene continental flood basalts, are present between 2-3 km  
557 depth below the seabed and represent the shallowest extrusive volcanics within the  
558 basin. The observed seismic amplitude character of the top of the extrusive pile in  
559 the Yolla-1 well can be compared with top extrusive volcanics in the Tobermory well  
560 in the Faroe-Shetland Basin (Fig. 17). Both Yolla-1 and Tobermory have around ~3  
561 km of sediment overlying the top of the extrusive volcanic pile and both encountered  
562 gas-bearing sandstones in the overlying sedimentary succession. The Tobermory  
563 example is typical of the top of the extrusive volcanic pile along the North Atlantic  
564 continental margin, which are generally associated with a very bright, hard kick. In  
565 contrast, in Yolla within the Bass Basin the top of the volcanics is a relatively dim hard  
566 kick. There are two significant features of contrast between Yolla and Tobermory.  
567 Firstly, there is an abundance of high-impedance EVCN coals in the strata overlying  
568 the Yolla subaerial volcanic rocks which, as already noted, also likely affects  
569 transmission of seismic energy and this imaging of the igneous intrusions within the  
570 Bass Basin. High impedance coals are not present in the strata at Tobermory.  
571 Secondly, the average sonic velocity of the sediments overlying the extrusive  
572 volcanics in Yolla is markedly higher ( $3975 \text{ m/s}$ ;  $77 \text{ ms ft}^{-1}$ ) than comparative  
573 sediments in Tobermory ( $3031 \text{ m/s}$ ;  $101 \text{ ms ft}^{-1}$ ). This significantly means the acoustic  
574 impedance contrast between the subaerial extrusive volcanics and the overlying  
575 sedimentary rocks within the Bass Basin is not as high as the extrusive volcanics  
576 within the Faroe-Shetland Basin. Ultimately a relatively dim hard kick could easily be  
577 misinterpreted as a subtle increase in acoustic impedance between two different

578 lithostratigraphic successions (e.g. between Middle and Lower EVCM in the case of  
579 the Bass Basin).

580         6.2. *Implications for exploration in other sedimentary basins affected by*  
581             *volcanism*

582 Based on our analysis of well and seismic data in the Bass Basin, we highlight three  
583 key factors that have generic implications for exploration of other sedimentary basins  
584 affected by magmatism:

585         1. ***Importance of understanding the geophysical properties of igneous***  
586             ***rocks as well as sedimentary host rock properties.*** The igneous  
587 intrusions within the Bass Basin are hosted within predominantly terrestrial  
588 sediments such as siltstone, coals and sandstones, in contrast to the  
589 relatively homogenous marine claystones typical of the North Atlantic  
590 Margin (e.g. Faroe-Shetland Basin). Consequently, the acoustic impedance  
591 of the Bass Basin intrusions is markedly lower than often associated with  
592 intrusions in basins such as the Faroe-Shetland basin. The presence of high  
593 impedance/low transmission coals, in particular, makes imaging of the  
594 underlying igneous intrusions and extrusive terrestrial lava facies more  
595 challenging. The variability in acoustic impedance of igneous rocks is an  
596 important factor to consider in basins where igneous material may be  
597 present in multiple sequences, such as the syn-rift lacustrine and post-rift  
598 marine strata of the Santos Basin, South Atlantic continental margin  
599 (Moreira et al. 2007).



- 600           2. **Integration of outcrop in the absence of nearby offset wells.** The  
601           Tasmanian Devil-1 well provides an illustrative example of how the  
602           examination of the nearest outcrop (extrusive volcanic in character) can  
603           help inform pre-drill seismic interpretation. This is an important aspect for  
604           exploration of basins where there may be little, if any, well control though  
605           outcrop is present, for instance within the flexural margins of half grabens  
606           along the East African Rift (Davison & Steel 2018).
- 607           3. **Knowledge transfer.** The Bass Basin shares similarities to the Rockall  
608           Trough, located along the North Atlantic continental margin, in that both  
609           basins have been affected by volcanism and exploration within them has  
610           occurred in distinct cycles (Schofield et al. 2017). Clearly a detailed audit,  
611           including forensic examination of geological end of well reports and pre-  
612           drill stratigraphic predictions, is important when exploring in basins  
613           impacted by magmatism to ensure accurate pre-drill interpretation of  
614           igneous units.

615

## 616           **7. Conclusions**

617           A consistent factor in the five decade-history of petroleum exploration in the Bass  
618           Basin, Australia, is the poor track record of explorers in predicting the presence of  
619           igneous rocks prior to drilling; of the 20 exploration wells where igneous rocks were  
620           intersected, in 13 instances those igneous rocks were not anticipated pre-drill (65%).  
621           This study has specifically investigated several of these exploration wells throughout

622 the Bass Basin, where the unanticipated presence of igneous rocks had profound  
623 implications for hydrocarbon prospectivity. In four instances (e.g. Tasmanian Devil-1),  
624 the prognosed primary reservoir target was found to be high-amplitude igneous  
625 rocks instead of clastic hydrocarbon-bearing reservoirs.

626 Through holistic examination of these wells, there appears to be three  
627 important factors contributing to poor pre-drill prediction of igneous rocks: (1) data  
628 quality and availability, (2) transfer of knowledge, and (3) the unique geology of the  
629 Bass Basin. Early on in the basin exploration history explorers were hindered by a lack  
630 of well control, and prospects were mapped on sparse, low quality 2D seismic lines.  
631 Nevertheless, even in modern seismic data a number of the volcanic units,  
632 particularly igneous intrusions, exhibit only moderately high acoustic impedance,  
633 compared to the very high acoustic impedance of similar intrusions in other  
634 sedimentary basins (e.g. the Faroe Shetland Basin). Generic lessons relevant to other  
635 sedimentary basins with volcanic histories include the importance of integrating  
636 available outcrop data in the absence of reliable well control, as well as  
637 understanding the geophysical properties of both the volcanics and the surrounding  
638 sedimentary strata when attempting to predict seismic properties.

639

#### 640 **Acknowledgements**

641 This work was carried out during a research visit to the Australian School of  
642 Petroleum at the University of Adelaide, and forms part of the lead author's PhD  
643 research, which is funded by a University of Aberdeen College of Physical Sciences  
644 Scholarship. Seismic interpretation was conducted using IHS Kingdom, and well log

645 interpretation using Schlumberger Techlog software. Synthetic seismic response  
646 modelling was performed using Ikon RokDoc software. This paper greatly benefited  
647 from the reviews of Sverre Planke, Kamal'deen Omosanya and an anonymous  
648 reviewer.

649

## 650 **References**

651 Archer, S.G., Bergman, S.C., Iliffe, J., Murphy, C.M., Thornton, M., 2005. Palaeogene  
652 igneous rocks reveal new insights into the geodynamic evolution and petroleum  
653 potential of the Rockall Trough, NE Atlantic Margin. *Basin Res.* 17, 171-201.

654 Alves, T., Omosanya, K. O., Gowling, P., 2015. Volume rendering of Enigmatic High  
655 Amplitude Anomalies (EHAA) in SE Brazil: A new method used in the analysis of fluid-  
656 flow and volcanic features. *Interpretation*, 3 (2), A1-A14.

657

658 Baillie, P.W., 1993. Regional geology. In: Maung, T.U., Miyazaki, S., Baillie,  
659 P.W., Laving, I.H., Vuckovic, V., Stephenson, A.E., Williamson, P.E., Staunton, J., Radke,  
660 S.G., West, B.W., Gippsie, R.G., Resiak, E., Temple, P.R. (Eds.), Eastern Bass Basin  
661 Petroleum Prospectivity Bulletin. Bureau of Resource Sciences.

662

663 Bartetzko, A., Delius, H., Pechinig, R., 2005. Effect of compositional and structural  
664 variations on log responses of igneous and metamorphic rocks I: mafic rocks. In:  
665 Harvey, P.K., Brewer, T.S., Pezard, P.A. & Petrov, V.Y. (eds) *Petrophysical Properties of*  
666 *Crystalline Rocks*. Geo. Soc. London. Spec. Pub., 240, 255-278.

667 Blevin, J.E., 2003. Petroleum Geology of the Bass Basin, Interpretation Report, an  
668 Output of the Western Tasmanian Regional Minerals Program. Geoscience Australia  
669 Record 2003/19.

670 Blevin, J.E., Cathro, D.L., 2008. Australian Southern Margin Synthesis, Project GA707.  
671 Client Report to Geoscience Australia by FrOG Tech Pty Ltd.

672 Blevin, J.E., Trigg, K.R., Partridge, E.D., Boreham, C.J., Lang, S.C., 2005.  
673 Tectonostratigraphy and potential source rocks of the Bass Basin. *APPEA J.* 45,  
674 601e622.

675 Boldreel, L. O., 2006. Wire-line log-based stratigraphy of flood basalts from the  
676 Lopra-1/1A well, Faroe Islands. *Geol. Surv. Den. Greenl. Bull.* 9, 7-22.

- 677 Boreham, C.J., Blevin, J.E., Duddy, I.R., Newman, J., Liu, K., Middleton, H., MacPhail,  
678 M.K., Cook, A.C., 2002. Exploring the potential for oil generation, migration and  
679 accumulation in Cape Sorell-1, Sorell Basin, offshore West Tasmania. *APPEA J.* 42,  
680 405e437.
- 681 Christopherson, K., 2016. The Greater Etom Area (GEA): A New Phase of Exploration  
682 in the South Lokichar Basin, Turkana County, Northern Kenya. *Africa Energy &*  
683 *Technology Conference.*
- 684 Coulombe, C. A. & Bird, D. N., 1996. Transmission filtering by high-amplitude  
685 reflection coefficients: Theory, practice, and processing considerations. *The Leading*  
686 *Edge*, 15 (9), 1037-1042.
- 687 Cummings, A.M., Hillis, R.R., Tingate, P.R., 2004. New perspectives on the structural  
688 evolution of the Bass Basin: implications for petroleum prospectivity. In: Boulton, P.J.,  
689 Johns, D.R., Lang, S.C. (Eds.), *Eastern Australian Basins Symposium II. PESA Special*  
690 *Publication*, 133-149.
- 691 Davison, I. & Steel, I. 2018. Geology and hydrocarbon potential of the East African  
692 continental margin: a review. In: *Tectonics and petroleum systems of East Africa*, *Pet.*  
693 *Geoscience*, 24,
- 694 Davies, R. Bell, B. R., Cartwright, J. A., Shoulders, S. 2002. Three-dimensional seismic  
695 imaging of Paleogene dike-fed submarine volcanoes from the northeast Atlantic  
696 margin. *Geology*, 30 (3), 223-226.
- 697 Delpino, D.H., Bermúdez, A.M., 2009. Petroleum systems including unconventional  
698 reservoirs in intrusive igneous rocks (sills and laccoliths). *The Leading Edge*, 28 (7),  
699 804-811.
- 700 Duddy, I.R., 2003. Mesozoic: a time of change in tectonic regime. In: Birch, W.D. (Ed.),  
701 *Geology of Victoria. Special Publication*, 23. Geological Society of Australia, Victoria  
702 Division, 239–286. Ch. 9
- 703 Dunlap, J., 2003. *40Ar/39Ar Dating of Minerals and Whole Rock from the Bass Basin.*  
704 *Research School of Earth Sciences, Australian National University for Geoscience*  
705 *Australia.*
- 706 Eide, C.H., Schofield, N., Jerram, D.A., Howell, J.A., 2017. Basin-scale architecture of  
707 deeply emplaced sill complexes: Jameson Land, East Greenland. *J. Geol. Soc.* 174 (1),  
708 23–40.

- 709 Faustmann, C., 1995. The Seismic Expression of Volcanism in the Bass Basin Referring  
710 to Western Victorian Analogues. University of Adelaide unpublished.
- 711 Gernigon, L., Ringenbach, J.C., Planke, S., Le Gall, B., 2004. Deep structures and  
712 breakup along volcanic rifted margins: Insights from integrated studies along the  
713 outer Vøring Basin (Norway). *Mar. and Pet. Geo.*, 21, 363-372
- 714 Grove, C. 2014. Direct and indirect effects of flood basalt volcanism on reservoir  
715 quality sandstone. PhD thesis, Durham University, UK.
- 716 Hardman, J., Schofield, N., Jolley, D., Hartley, A., Holford, S. & Watson, D., 2018.  
717 Controls on the distribution of volcanism and intra-basaltic sediments in the Cambo-  
718 Rosebank region, West of Shetland. *Pet. Geo.* **xx**, xxx-xxx,  
719 <https://doi.org/10.1144/petgeo2017-061>
- 720 Hansen, J-A., Bergh, S. G., Henningsen, T., 2011. Mesozoic rifting and basin evolution  
721 on the Lofoten and Vesterålen Margin, North-Norway; time constraints and regional  
722 implications. *Norw. J. Geo.*, 91, 203-228.
- 723 Holford, S.P., Hillis, R.R., Duddy, I.R., Green, P.F., Stoker, M.S., Tuitt, A.K., Backe, G.,  
724 Tassone, D.R., MacDonald, J.D., 2011. Cenozoic post-breakup compressional  
725 deformation and exhumation of the southern Australian margin. *APPEA J.* 51, 613-  
726 638.
- 727 Holford, S.P., Schofield, N., Macdonald, J.D., Duddy, I.R., Green, P.F., 2012. Seismic  
728 analysis of igneous systems in sedimentary basins and their impacts on hydrocarbon  
729 prospectivity: examples from the southern Australian margin. *APPEA J.* 52, 229-252.
- 730 Holford, S.P., Schofield, N., Jackson, C.A.L., Magee, C., Green, P.F., Duddy, I.R., 2013.  
731 Impacts of Igneous Intrusions on Source and Reservoir Potential in Prospective  
732 Sedimentary Basins along the Western Australian Continental Margin. In: Keep, M.,  
733 Moss, S.J. (Eds.). *The Sedimentary Basins of Western Australia IV*, Perth. Holford, S.P.,  
734 Schofield, N., Macdonald, J.D., Duddy, I.R., Green, P.F., 2012. Seismic analysis of  
735 igneous systems in sedimentary basins and their impacts on hydrocarbon  
736 prospectivity: examples from the southern Australian margin. *APPEA J.* 52, 229-252.
- 737 Holford, S.P., Tuitt, A.K., Hillis, R.R., Green, P.F., Stoker, M.S., Duddy, I.R., Sandiford, M.,  
738 Tassone, D.R., 2014. Cenozoic deformation in the Otway Basin, southern Australian  
739 margin: implications for the origin and nature of postbreakup compression at rifted  
740 margins. *Basin Res.* 26, 10-37.

- 741 Holford, S. P., Schofield, N., Reynolds, P. Subsurface fluid flow focused by buried by  
742 volcanoes in sedimentary basins: Evidence from 3D seismic data, Bass Basin, offshore  
743 southeastern Australia. *Interp.* 5, 39-50.
- 744 Jackson, C.A.-L., Schofield, N., Golenkov, B., 2013. Geometry and controls on the  
745 development of igneous sill-related forced folds: A 2-D seismic reflection case study  
746 from offshore southern Australia. *Geo. Soc. America. Bull.* 125, 1874-1890.
- 747 Jerram, D. A., Widdowson, M. 2005. The anatomy of Continental Flood Basalt  
748 Provinces: geological constraints on the processes and products of flood volcanism.  
749 *Lithos.* 79, 385-405.
- 750 Jolley, D.W., Bell, B.R., 2002. Genesis and age of the Erlend volcano, NE Atlantic  
751 margin. *Geol. Soc. Lond. Spec. Publ.* 197 (1), 95-109.
- 752 Le Bas, M.J., Lemaitre, R.W., Streckeisen, A. and Zanettin, B. (1986). A Chemical  
753 Classification of Volcanic-Rocks Based on the Total Alkali Silica Diagram. *J. Petrology.*  
754 27 (3), 745-750.
- 755 Lennon, R.G., Suttill, R.J., Guthrie, D.A., Waldron, A.R., 1999. The renewed search for  
756 oil and gas in the Bass Basin: results of Yolla-2 and White Ibis-1. *APPEA J.* 39,  
757 248e262.
- 758 Loizou, N. 2014. Success in exploring for reliable, robust Paleocene traps west of  
759 Shetland. *In: Cannon, S. J. C. & Ellis, D. (eds). Hydrocarbon Exploration to Exploitation*  
760 *West of Shetlands. Geol. Soc, London, Spec. Pub., 397, 59-79.*
- 761 Magee, C., Maharaj, S. M., Wrona. T., Jackson CA-L., 2015. Controls on the expression  
762 of igneous intrusions in seismic reflection data. *Geosphere*, 11, 1024-1041
- 763 Mark, N. J., Schofield, N., Pugliese, S., Watson, D., Holford, S., Muirhead, D., Brown, R.,  
764 Healy, D., 2017. Igneous intrusions in the Faroe Shetland basin and their implications  
765 for hydrocarbon exploration; new insights from well and seismic data.  
766 <https://doi.org/10.1016/j.marpetgeo.2017.12.005>
- 767 Mathisen, M. E., McPherson, J. G., 1991. Volcaniclastic deposits: implications for  
768 hydrocarbon exploration. *Sedimentation in Volcanic Settings, SEPM Special*  
769 *Publications.* 45, 27-36.

- 770 McLean, C. E., Schofield, N., Brown, D. J., Jolley, D. W., Reid, A., 2017. 3D seismic  
771 imaging of the shallow plumbing system beneath the Ben Nevis Monogenetic  
772 Volcanic Field: Faroe-Shetland Basin. *J. Geol. Soc.* 174 (3), 468-485.
- 773 Meeuws, F. J. E., Holford, S. P. Foden, J. D., Schofield, N. 2016. Distribution,  
774 chronology and causes of Cretaceous-Cenozoic magmatism along the magma-poor  
775 rifted southern Australian margin: Links between mantle melting and basin  
776 formation. *Mar. Petroleum Geol.* 73, 271-298.
- 777 Millet, J. M., Wilkins, A. D., Campbell, E., Hole, M. J., Taylor, R. A., Healy, D., Jerram, D.  
778 A., Jolley, D. W., Planke, S., Archer, S. G., Blischke, A. 2016. The geology of offshore  
779 drilling through basaltic sequences: Understanding operational complications to  
780 improve efficiency. *Mar. Petroleum Geo.* 77, 1177-1192.
- 781 Mjelde, R., Raum, T., Murai, Y., Takanami, T., 2007. Continent-ocean-transitions:  
782 Review, and a new tectono-magmatic model of the Voring Plateau, NE Atlantic. *J.*  
783 *Geodynamics*, 43, 374-392.
- 784  
785 Moore, J.G., 2001. Density of basalt core from Hilo drill hole, Hawaii. *J. Vol. Geo. Res.*  
786 112, 221-230.
- 787  
788 Moreira, J. L. P., Madeira, C. V., Gil, J. A., Machado, M. A., P., 2007. Bacia de Santos.  
789 *Boletim de Geociências da Petrobras, Rio de Janeiro.* 15, 531-549.
- 790 Nelson, C. E., Jerram, D. A., Hobbs, R. W. 2009. Flood basalt facies from borehole data:  
791 implications for prospectivity and volcanology in volcanic rifted margins. *Pet.*  
792 *Geoscience.* 15, 313-324.
- 793 O'Halloran, G., Johnstone, E., 2001. Late Cretaceous rift volcanics of the Gippsland  
794 Basin, SE Australia e new insights from 3D seismic. In: Hill, K.C., Bernecker, T. (Eds.),  
795 *Eastern Australasian Basins Symposium: a Refocussed Energy Perspective for the*  
796 *Future.* Petroleum Exploration Society of Australia, Melbourne, Victoria, 353-361.
- 797 Palmowski, D., Hill, K.C., and Hoffman, N., 2004. Structure and hydrocarbons in the  
798 Shipwreck Trough, Otway Basin: half-graben gas fields abutting a continental  
799 transform.  
800 *APPEA Journal*, v. 44, 417-440.
- 801  
802 Planke, S., 1994. Geophysical response of flood basalts from analysis of wire line logs:  
803 Ocean Drilling Program Site 642, Vøring volcanic margin. *Journal of Geophysical*  
804 *Research: Solid Earth.* 99, 9279-9296.
- 805



- 806 Planke, S., Symonds, P.A., Alvestad, E., and Skogseid, J., 2000. Seismic  
807 volcanostratigraphy of large-volume basaltic extrusive complexes on rifted margins.  
808 *J. Geophysical Research-Solid Earth*, v. 105, p. 19335- 19351.
- 809 Planke, S, Rasmussen, T.E., Rey, S.S., Myklebust, R., 2005. Seismic characteristics and  
810 distribution of volcanic intrusions and hydrothermal vent complexes in the Vøring  
811 and Møre basins. In: Doré, A.G. & Vining, B. (eds) *Petroleum Geology: North-West*  
812 *Europe and Global Perspectives- Proceedings of the 6th Petroleum Geology*  
813 *Conference*, 84, 1-12.
- 814 Poppitt, S., Duncan, L.J., Preu, B., Fazzari, F. & Archer, J., 2016. The influence of  
815 volcanic rocks on the characterization of Rosebank Field–new insights from ocean-  
816 bottom seismic data and geological analogues integrated through interpretation and  
817 modelling. In: Bowman, M. & Levell, B. (eds) *Petroleum Geology of NW Europe: 50*  
818 *Years of Learning – Proceedings of the 8th Petroleum Geology*
- 819 Purcell, P. G. 2017. Re-imagining and re-imaging the development of the East African  
820 Rift. In: *Tectonics and Petroleum Systems of East Africa. Petroleum Geoscience*, 24,  
821 21-40. <https://doi.org/10.1144/petgeo2017-036>
- 822 Rabbel, O., Galland, O., Mair, K., Lecomte, I., Senger, K., Spacapan, J. B., Manceda, R.,  
823 2018. From field analogues to realistic seismic modelling: a case study of an oil-  
824 producing andesitic sill complex in the Neuquén Basin, Argentina. *J. Geol. Soc.* First  
825 published online 2<sup>nd</sup> March <https://doi.org/10.1144/jgs2017-116>
- 826 Rateau, R., Schofield, N., Smith, M., 2013. The potential role of igneous intrusions on  
827 hydrocarbon migration, West of Shetland. *Pet. Geosci.* 19, 259–272.
- 828 Reynolds, P., Schofield, N., Brown, R. J., Holford, S. P., 2018. The architecture of  
829 submarine monogenetic volcanoes- insights from 3D seismic data. *Basin Res.* 30,  
830 437-451.
- 831 Schofield, N., Holford, S., Millet, J., Brown, D., Jolley, D., Passey, S.R., Muirhead, D.,  
832 Grove, C., Magee, C., Murray, J., Hole, M., Jackson, C.A.-L., Stevenson, C., 2015.  
833 Regional magma plumbing and emplacement mechanisms of the Faroe-Shetland Sill  
834 Complex: implications for magma transport and petroleum systems within  
835 sedimentary basins. *Basin Res.* 19 first published online November. [http://doi.org/10.](http://doi.org/10.1111/bre.12164)  
836 [1111/bre.12164](http://doi.org/10.1111/bre.12164).
- 837 Schofield, N., Jolley, D., Holford, S., Archer, S., Watson, D., Hartley, A., Howell, J.,  
838 Muirhead, D., Underhill, J., Green, P., 2017. Challenges of future exploration within the



- 839 UK Rockall Basin. In: Geological Society, London, Petroleum Geology Conference  
840 Series, vol. 8. Geological Society of London, PGC8–37.
- 841 Schutter, S.R., 2003. Hydrocarbon occurrence and exploration in and around igneous  
842 rocks. *Geol. Soc. Lond. Spec. Publ.* 214 (1), 7–33.
- 843 Self, S., Thordarson, T., Keszthelyi, L., 1997. Emplacement of Continental Flood Basalt  
844 Lava Flows. In: Mahoney, J.J., Coffin, M.F. (Eds.) *Large Igneous Provinces: Continental,*  
845 *Oceanic, and Planetary Flood Volcanism.* AGU Monograph, 100, 381–410.
- 846 Serra, O., Baldwin, J., Quirein, J., 1980. Theory, Interpretation and Practical  
847 Applications of Nastral Gamma Ray Spectroscopy. SPWLA 21<sup>st</sup> Annual Logging  
848 Symposium, July 8-11, 1-30.
- 849 Sheriff, R.E. & Geldart, L.P., 1983. *Exploration Seismology Vol. 2: Data-Processing and*  
850 *Interpretation.* Cambridge University Press, Cambridge.
- 851 Single, R.T., Jerram, D.A., 2004. The 3D facies architecture of flood basalt provinces  
852 and their internal heterogeneity: examples from the Palaeogene Skye Lava Field.  
853 *J. Geol. Soc.* 161, 911–926.
- 854 Smallwood, J.R., Maresh, J., 2002. The properties, morphology and distribution of  
855 igneous sills: modelling, borehole data and 3D seismic data from the Faeroe-  
856 Shetland area. In: In: Jolley, D.W., Bell, B.R. (Eds.), *The North Atlantic Igneous Province:*  
857 *Stratigraphy, Tectonic, Volcanic and Magmatic Processes,* vol. 197. *Geol. Soc. London.*  
858 *Spec. Publ.,* 271–306.
- 859 Stagg, H.M.V., Cockshell, C.D., Willcox, J.B., Hill, A.J., Needham, D.V.L., Thomas, B.,  
860 O'Brien, G.W., Hough, L.P., 1990. Basins of the Great Australian Bight region, geology  
861 and petroleum potential. In: Bureau of Mineral Resources, A. (Ed.), *Continental*  
862 *Margins Program, Folio 5.*
- 863 Thomson, K., Schofield, N., 2008. Lithological and structural controls on the  
864 emplacement and morphology of sills in sedimentary basins, *Structure and*  
865 *Emplacement of High-Level Magmatic Systems.* *Geol. Soc. Lond. Spec. Publ.* 302, 31–  
866 44.
- 867 Trigg, K.R., Blevin, J.E., Boreham, C.J., 2003. In: Australia, G. (Ed.), *An Audit of*  
868 *Petroleum Exploration Wells in the Bass Basin 1965-1999.*
- 869 Walton, A.W., Schiffman, P., 2003. Alteration of hyaloclastites in the HSDP 2 Phase 1  
870 Drill Core 1. Description and paragenesis. *Geochemistry, Geophysics, Geosystems* 4  
871 (5).  
872

- 873 Watson, D., Schofield, N., Jolley, D., Archer, S., Finlay, A. J., Mark, N., Hardman, J.,  
874 Watton, T., 2017. Stratigraphic Overview of Palaeogene Tuffs in the Faroe-Shetland  
875 Basin, NE Atlantic Margin. *J. Geol. Soc.* 174 (4), 627-645.
- 876 Watton, T. J., Wright, K. A., Jerram, D. A. & Brown, R. J., 2014. The petrophysical and  
877 petrographical properties of hyaloclastite deposits: Implications for petroleum  
878 exploration. *AAPG Bull* 98 (3), 449-463.
- 879 Winchester, J. A. & Floyd, P. A., 1977. Geochemical discrimination of different magma  
880 series and their differentiation products using immobile elements. *Chem. Geo.* **20**,  
881 325-434

882

883

884

### 885 **Figure Captions**

886 **Fig. 1.** **a)** Main structural elements of the Bass Basin, adapted from Lennon et al.  
887 (1999) and Cummings et al. (2004), including **b)** the locations of exploration awells  
888 within the basin, and the location of figures shown in this study.

889 **Fig. 2.** Bass Basin stratigraphic nomenclature adopted in this paper, lithostratigraphy  
890 adapted from Lennon et al. 1999 and sequences from Cummings et al. 2004.

891 **Fig. 3.** Workflow for investigating micro-scale datasets used in this study, with an  
892 example from a core sample from the Aroo-1 well at 3596.2 m MD (11798.59 ft). The  
893 thin-section micrograph is courtesy of Geoscience Australia.

894 **Fig. 4.** Frankenstein well log demonstrating the log motif of different varieties of  
895 igneous lithologies in the subsurface. The log is constructed from real examples,  
896 from multiple wells from the North Atlantic Margin (references along the far right  
897 hand side). Mafic volcanic rocks generally exhibit low gamma values (**a**), whereas  
898 silicic rocks measure markedly higher values (**b**). Crystalline volcanic rocks such as  
899 basaltic compound lava flows (**c**), tabular lava flows (**d**) and igneous intrusions (**e**)  
900 have relatively high resistivity and low neutron porosity. Volcaniclastic rocks, such as  
901 tuffaceous rocks (**f**), intra-lava volcanic claystones (**g**) and hyaloclastite (**h**)  
902 demonstrate significantly higher neutron porosity and lower resistivity due to the  
903 presence of clay bound waters.

904 **Fig. 5.** Generalised igneous lithology seismic stratigraphy within the Bass Basin. The  
905 seismic datasets in this study are shown in time with a normal polarity, whereby a

906 downward increase in acoustic impedance produced a peak (a hard kick). Insets of  
 907 the three main types of igneous material are displayed, as well as the sea floor for  
 908 polarity reference. The top of the submarine volcanics is associated with a bright,  
 909 seismically resolvable hard kick. A number of the igneous intrusions are poorly  
 910 imaged, in this instance exhibiting a faint seismically identifiable hard ( ~2 secs TWT).  
 911 Finally, the top of the subaerial volcanics is generally associated with a moderately  
 912 bright, seismically resolvable hard.

913 **Fig. 6.** Frankenstein log depicting the igneous rocks encountered throughout the  
 914 Bass Basin. In terms of the submarine volcanic rocks, chiefly hyaloclastite, the log  
 915 motif is characterised by (a) continuously low gamma and (b) moderately high  
 916 resistivity. Whilst no bulk density log has been acquired through these hyaloclastites  
 917 in any of the wells, a density log can be derived from the sonic log, revealing a  
 918 relatively low bulk density (c). Overall the submarine hyaloclastite packages exhibit a  
 919 variably fast sonic velocity (d). With regards to the igneous intrusions encountered  
 920 within the Bass Basin, the largely dolerite material exhibits low gamma (e) and high  
 921 resistivity (f). The bulk density is generally high ( $>2.8 \text{ g cm}^{-3}$ ), except where poor hole  
 922 conditions lead to anomalously low values (g). These igneous intrusions exhibit fast  
 923 sonic velocity (h). However, within several wells a raft of higher gamma/lower density  
 924 silicic igneous material is recognised (i). Finally, in terms of the subaerial volcanic  
 925 rocks, a characteristic log motif of repeating blocks of low gamma (j), high resistivity  
 926 (k), high density/low neutron porosity (l) and fast sonic velocity (m) are typical of  
 927 tabular lava flows. Where the bulk density exhibits continuously marginally lower  
 928 values than the tabular lavas, this likely represents compound lava flows.

929 **Fig. 7.** Regional distribution of igneous rocks throughout the Bass Basin, as proven  
 930 by well penetrations (red outlined text boxes). Submarine volcanic are present within  
 931 the Angahook Formation within the Torquay Group. Igneous intrusions are hosted  
 932 predominantly within the Middle EVCM, with one penetration within the Upper  
 933 EVCM (Tilana-1 well, Dondu Trough). Subaerial volcanic rocks, finally, are present  
 934 within the Middle EVCM in the Cape Wickham Sub-basin, and in the Durroon  
 935 Formation within the Duroon Sub-basin (Anderson Trough). Seismic basin fill not  
 936 penetrated (dashed lines) based on Cummings *et al.* 2005.

937 **Fig. 8.** Core from a hyaloclastite succession from the Bass-1 well. Features of note  
 938 include (b) rounded grains denote a degree of sorting; (c) Fine-grained tuffaceous  
 939 and pumice clasts are also visible; (d) Normally graded beds.

940 **Fig. 9.** Distinct intrusion log profile recognised throughout the Bass Basin, whereby a  
941 more silicic raft of intrusive material is present in the upper third of the intrusion  
942 body, surrounded by dolerite. This magmatic contrast is supported by XRF  
943 geochemistry performed on ditch cuttings in two separate zones within the Seal-1  
944 well (yellow stippled area).

945 **Fig. 10.** Bass Basin exploration timeline showing wells where igneous rocks were not  
946 predicted pre-drill. A number of the early wells were drilled on spare, 2D seismic  
947 lines. Another important feature is the cyclical nature of exploration, where a new  
948 company would enter the basin, embark upon a drilling campaign and fail to predict  
949 the presence of igneous rocks. Similar unexpectedly encountered igneous were  
950 encountered within the contiguous Gippsland Basin (Sailfish-1 & Kipper-1 wells).

951 **Fig. 11.** Regional 2D seismic line through the Bass-1 well (offset wells greyed out to  
952 reflect they were drilled later). The build of material recognised on seismic was  
953 interpreted pre-drill as a carbonate reef, though turned out to be a submarine  
954 volcano. The lower images are geoschematic representations modified from the  
955 Bass-1 end of well report.

956 **Fig.12.** Predicted stratigraphy compared to encountered (actual) stratigraphy and  
957 lithologies within the Aroo-1 well.

958 **Fig. 13. A)** Tasmanian Devil-1 prospect within a regional 2D seismic context, where  
959 broad graben structure recognised. **B & C)** pre and post drill lithology columns,  
960 modified from the Tasmanian Devil-1 end of well report. The accompanying  
961 interpreted seismic

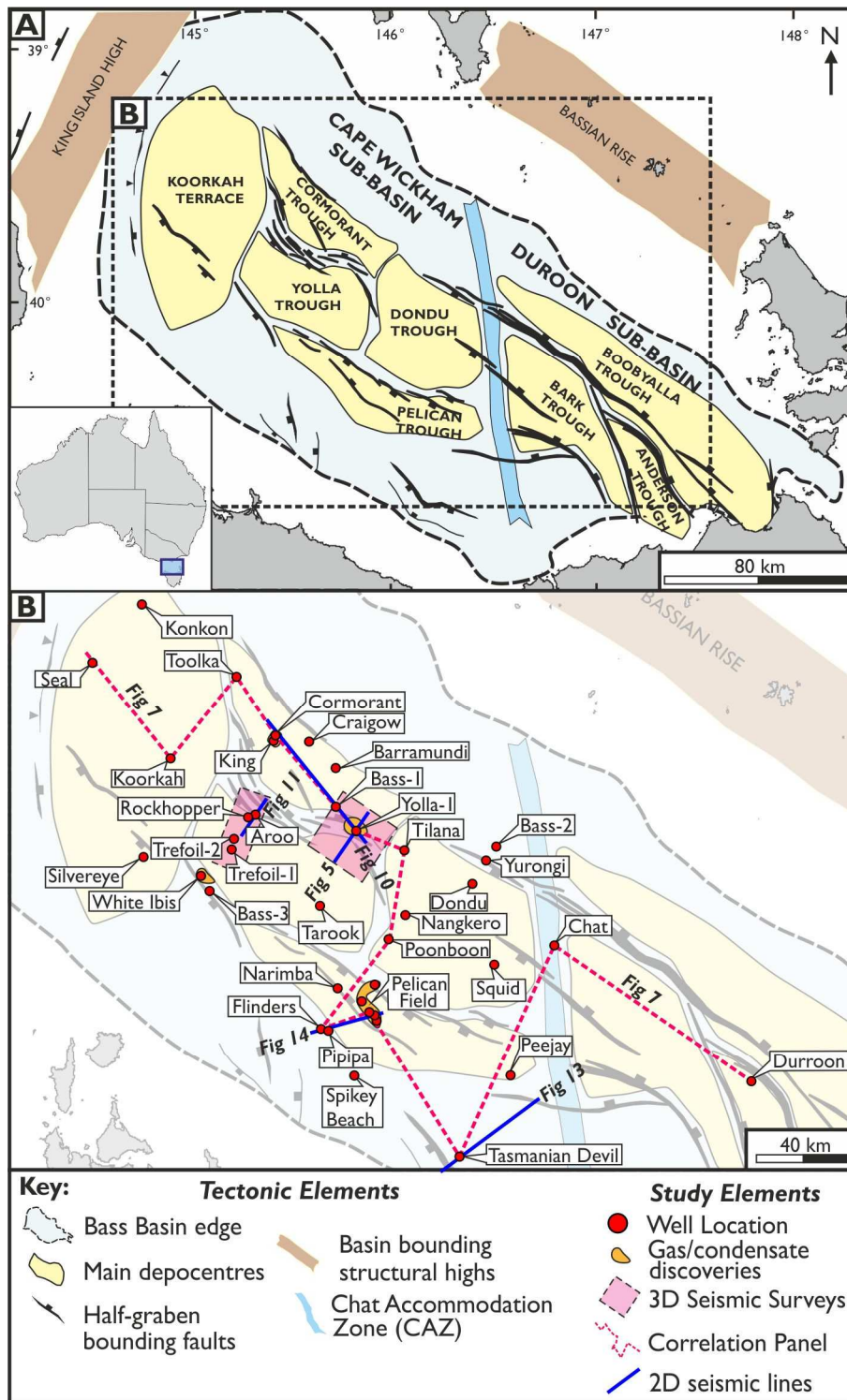
962 **Fig. 14.** Flinders-1 uninterpreted and interpreted seismic line (upper section). The  
963 pre-drill target was an amplitude anomaly at a slightly deeper level than where the  
964 Pipipa-1 offset well terminated. Upon drilling the amplitude anomaly was instead  
965 found to be a 64 m thick igneous intrusion, confirmed by modelling the synthetic  
966 response (lower section).

967 **Fig. 15.** Comparison between modern seismic data and the black and white seismic  
968 data in which the Flinders-1 prospect was interpreted on.

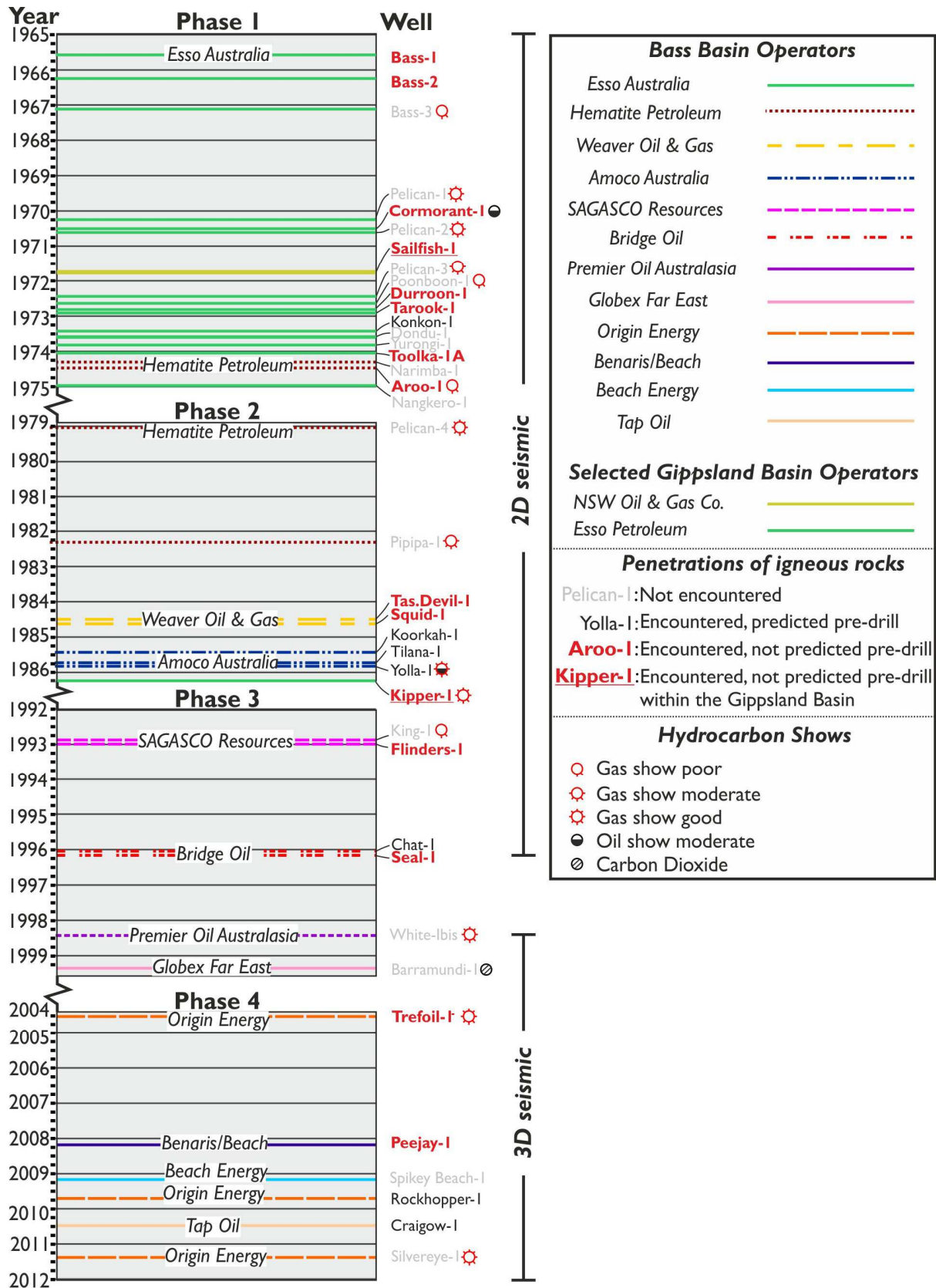
969 **Fig. 16.** Synthetic seismic comparison between intrusions from the FSB (from Mark et  
970 al. 2018) and the Bass Basin, Flinders-1 example (highlighted by dashed yellow lines  
971 on seismic). The FSB intrusion is not as thick and is present within deeper sediments  
972 than the Flinders-1 intrusion. However, a denser host rock and the presence of a raft  
973 of silicic material associated with the Flinders-1 intrusion combine to produce a

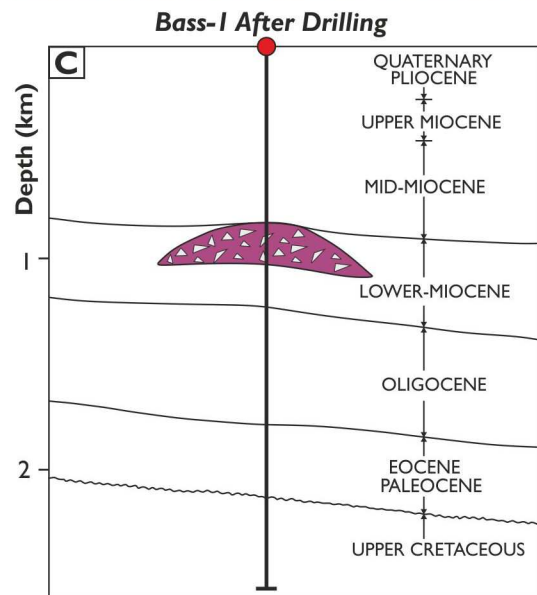
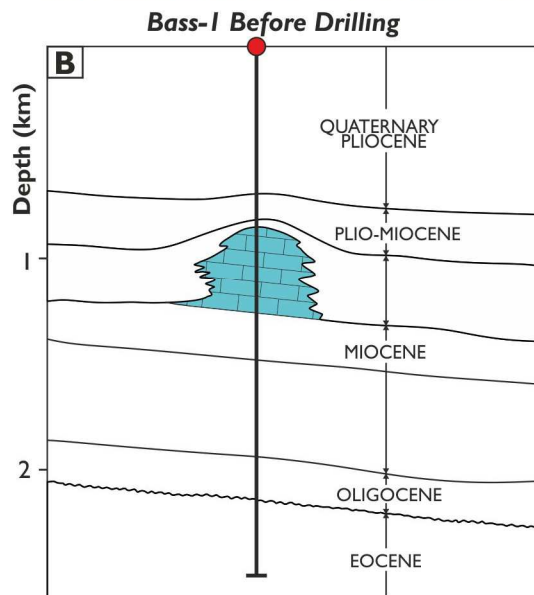
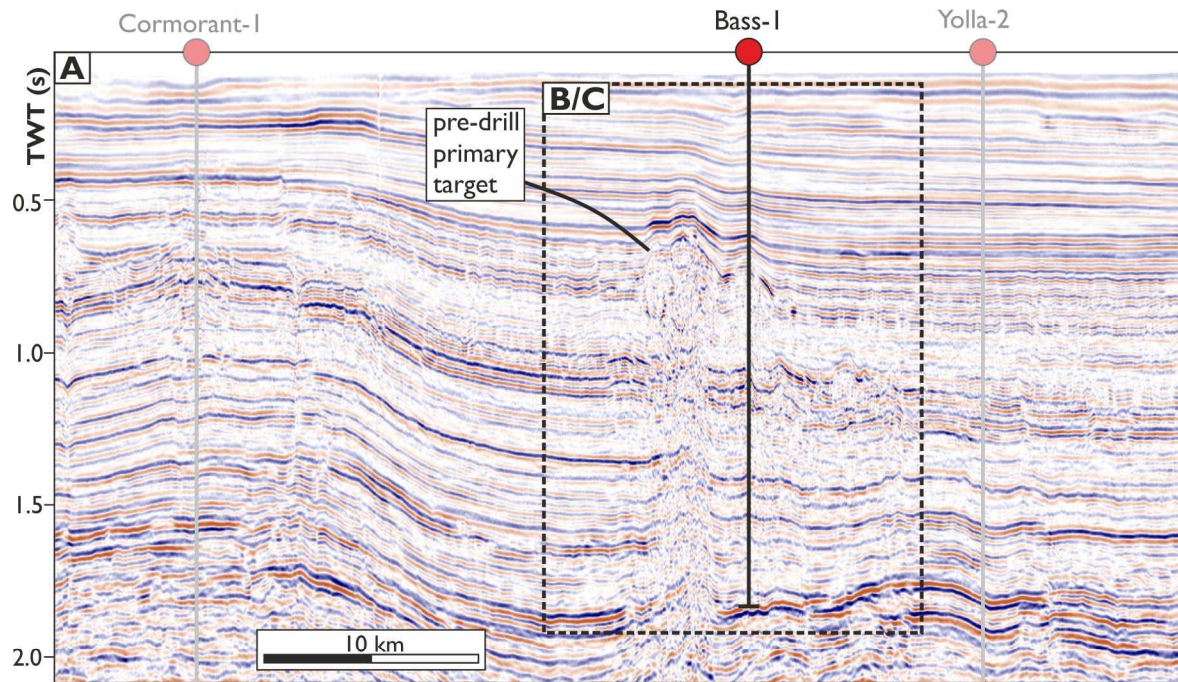
974 dimmer reflection. The presence of coals within the overburden also likely acts as a  
975 transmission filter, hindering imaging of the sediments and the intrusion below.

976 **Fig. 17.** Seismic comparison between top extrusive volcanics within the Bass Basin  
977 and the Faroe-Shetland Basin, North Atlantic Margin (seismic from the PGS FSB  
978 MegaSurvey Plus). The reflection associated with the top of the extrusive volcanics in  
979 the Bass Basin appears dimmer than the FSB equivalent due to the presence of high  
980 impedance coals acting as a transmission filter, and the overlying sediments being  
981 acoustically faster, hence a lower acoustic impedance is generated between the  
982 volcanics and the surrounding sedimentary rocks.

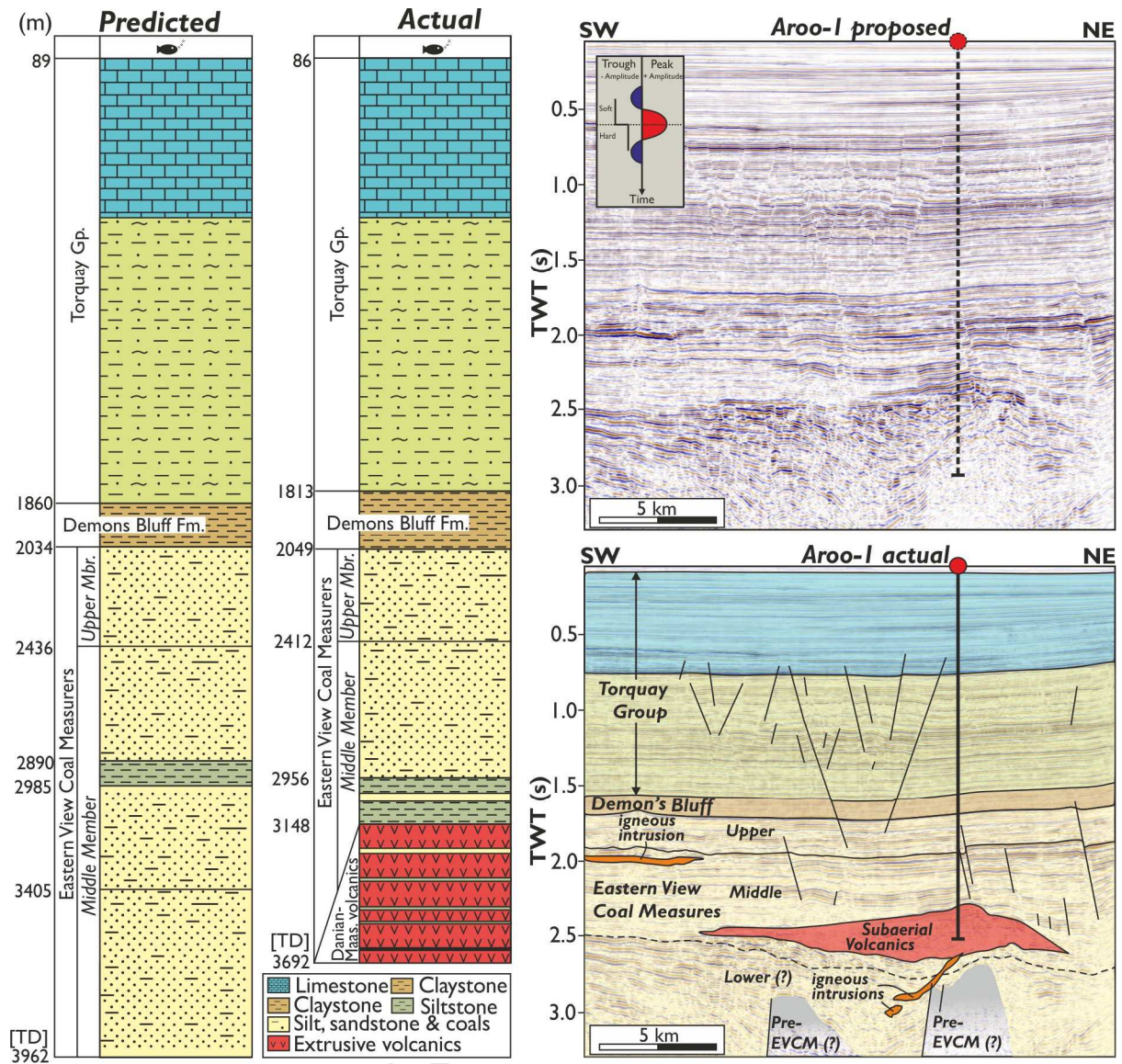




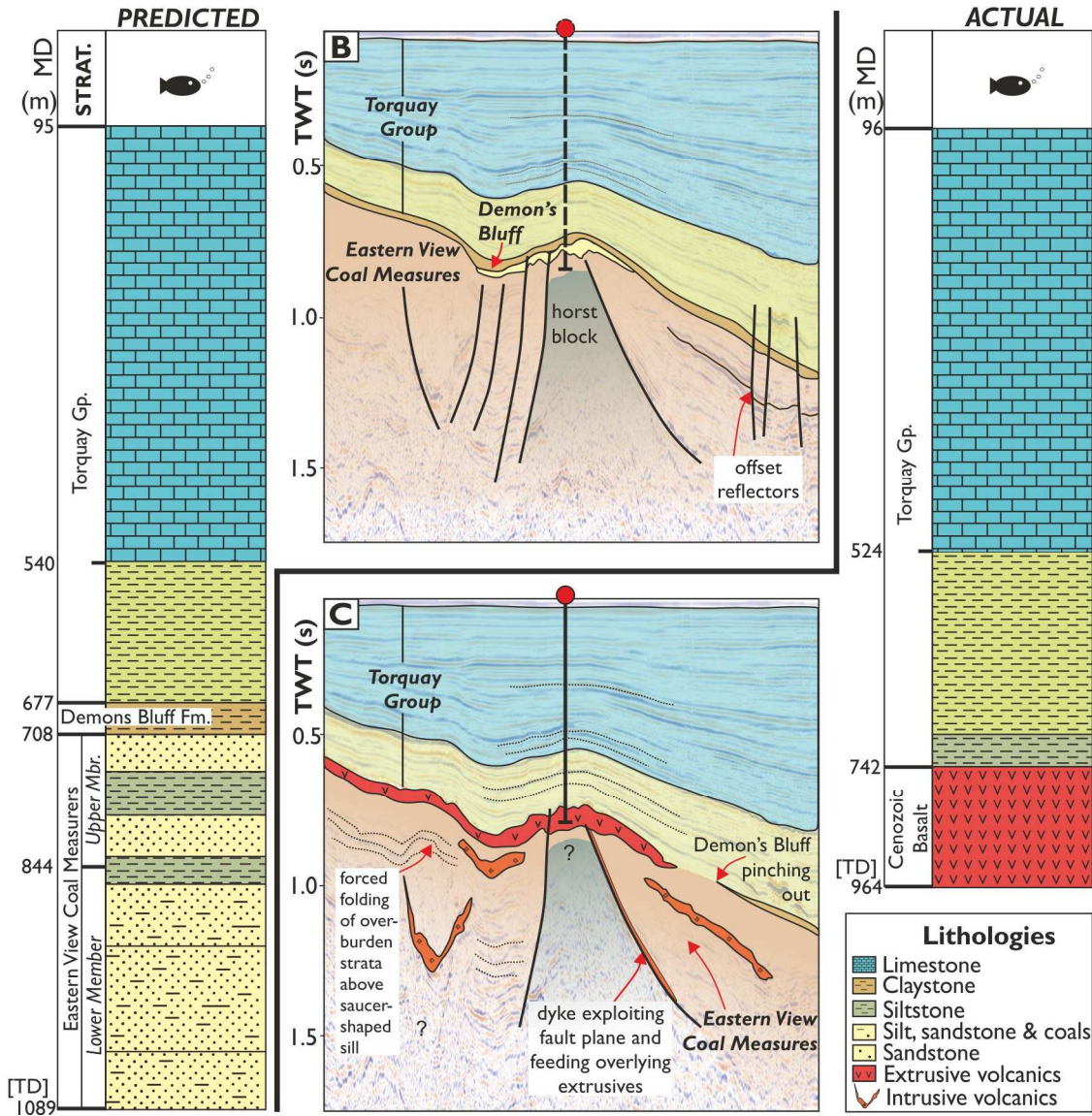
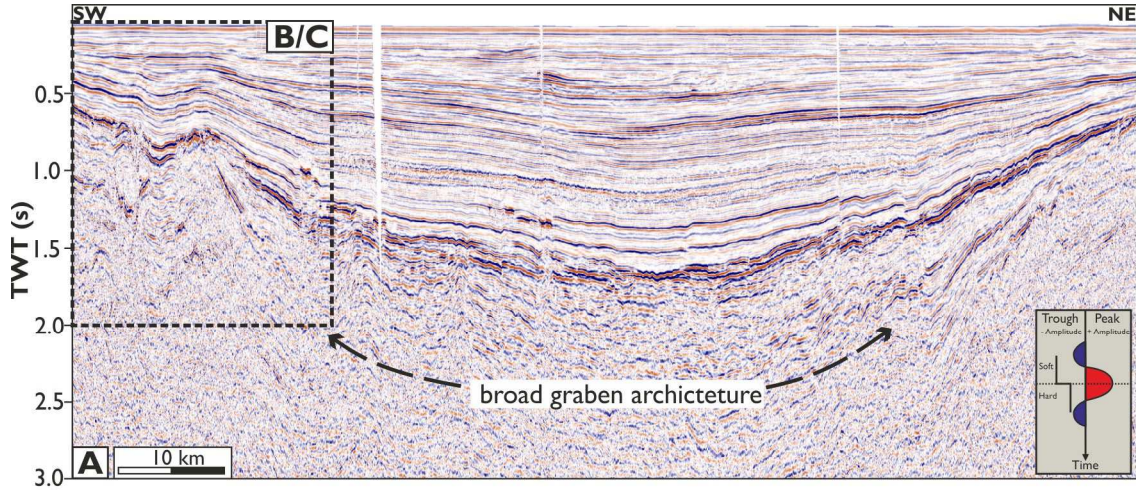




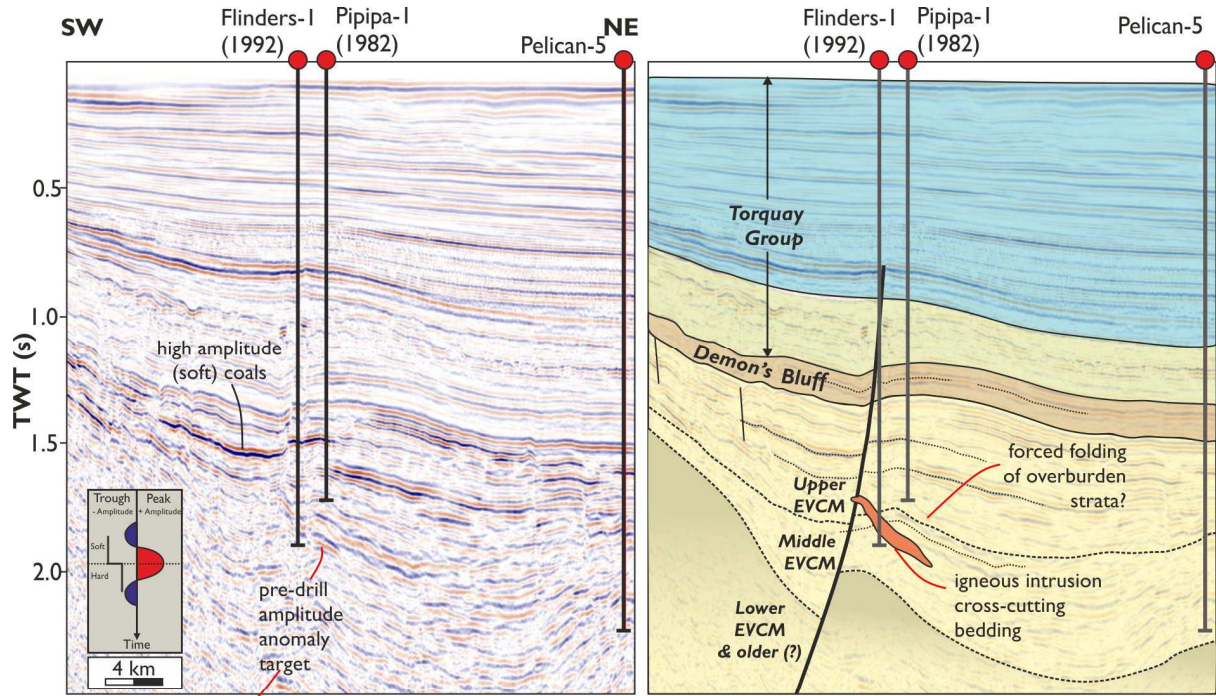




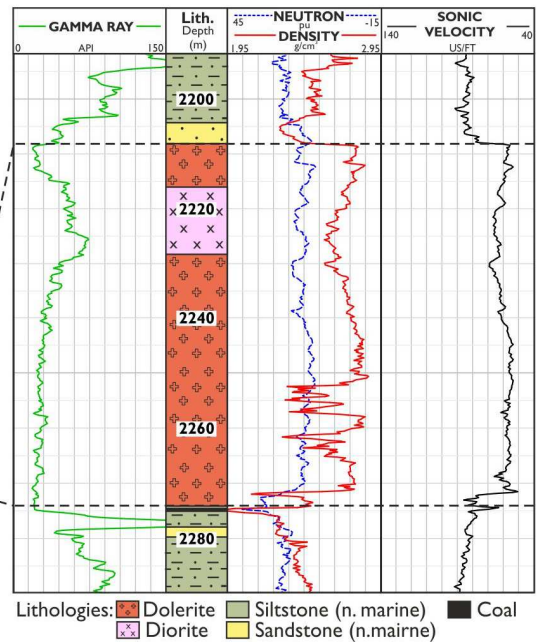
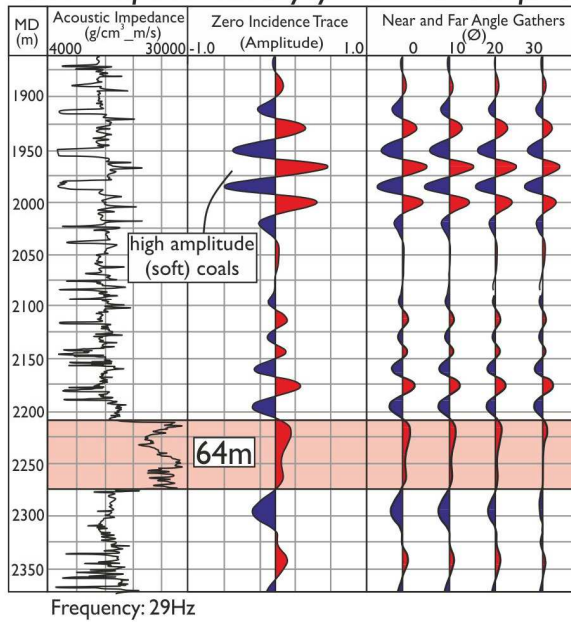




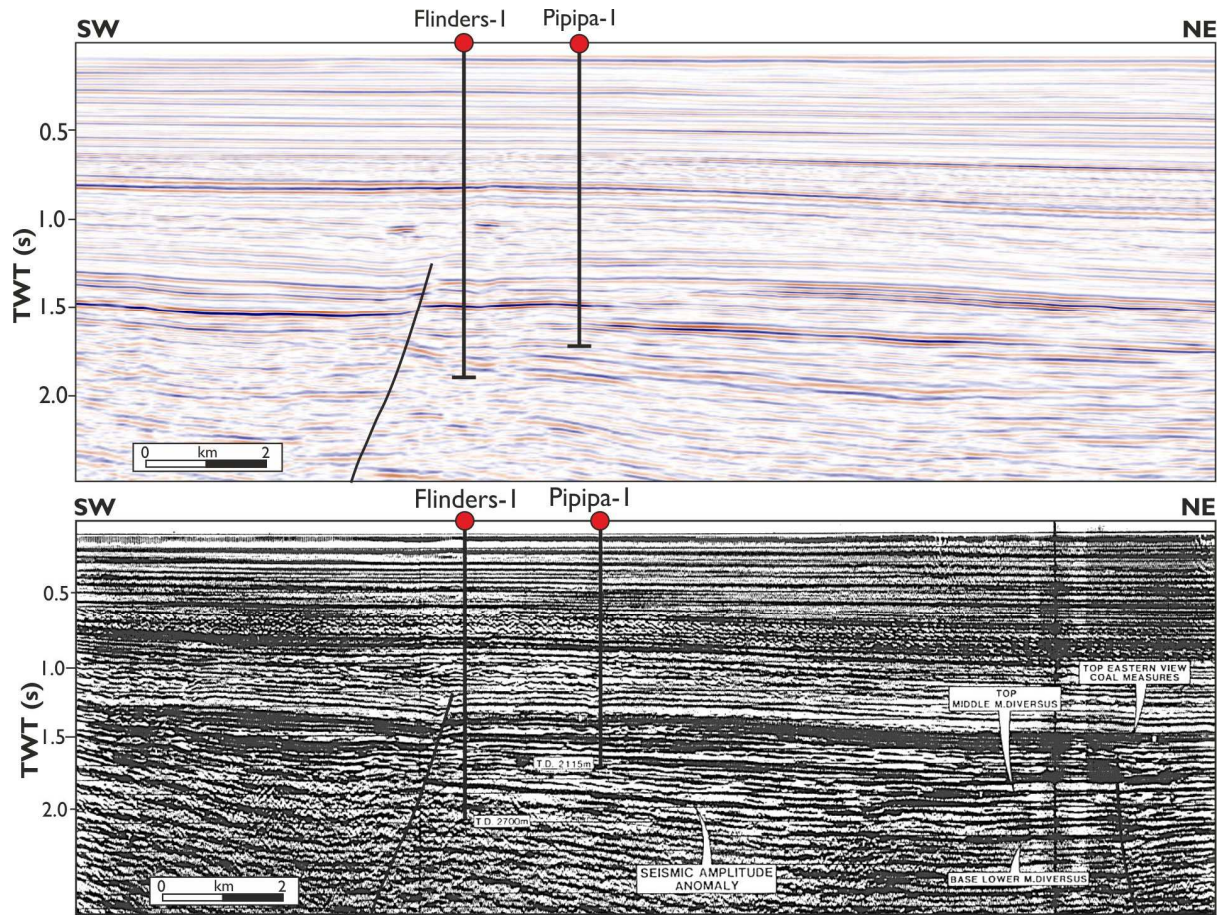




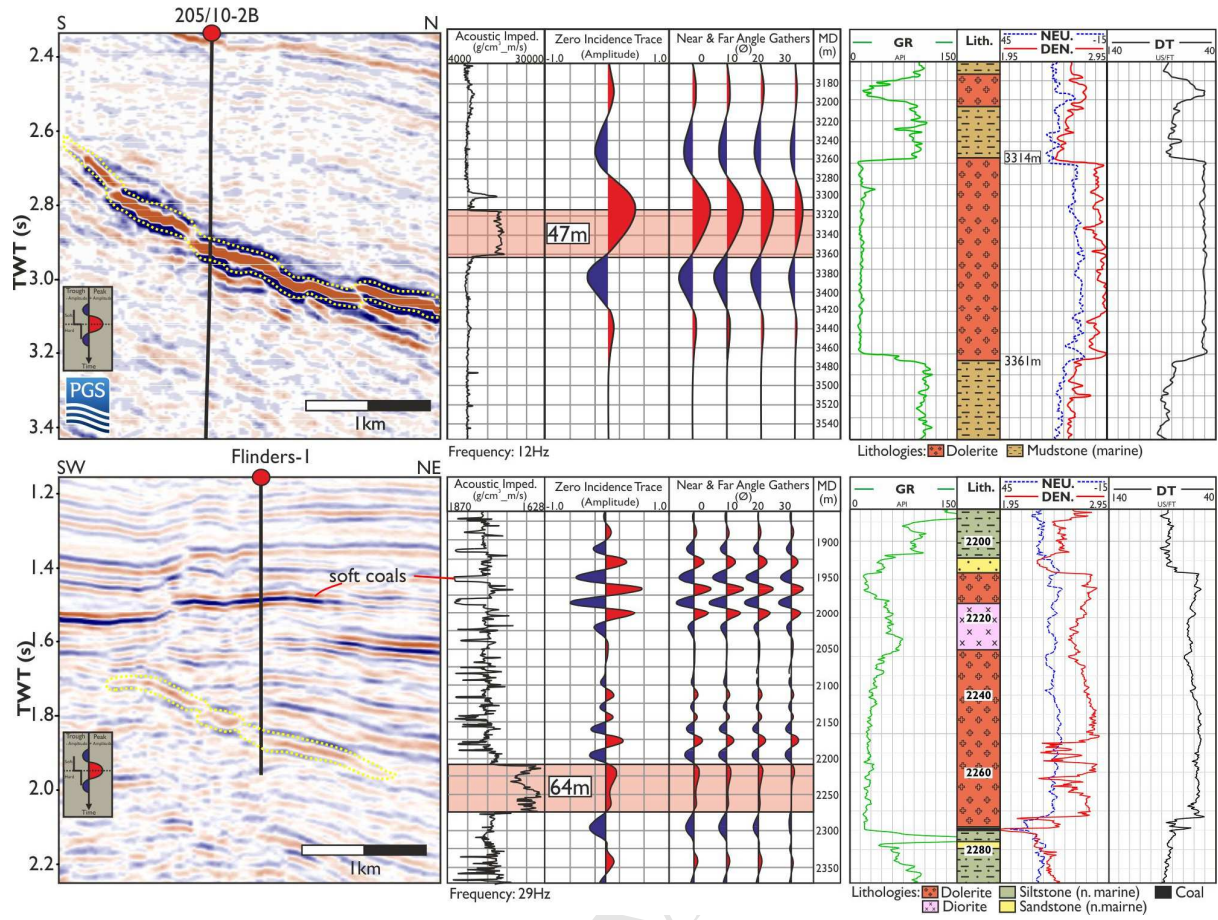
Pre-drill amplitude anomaly synthetic seismic response

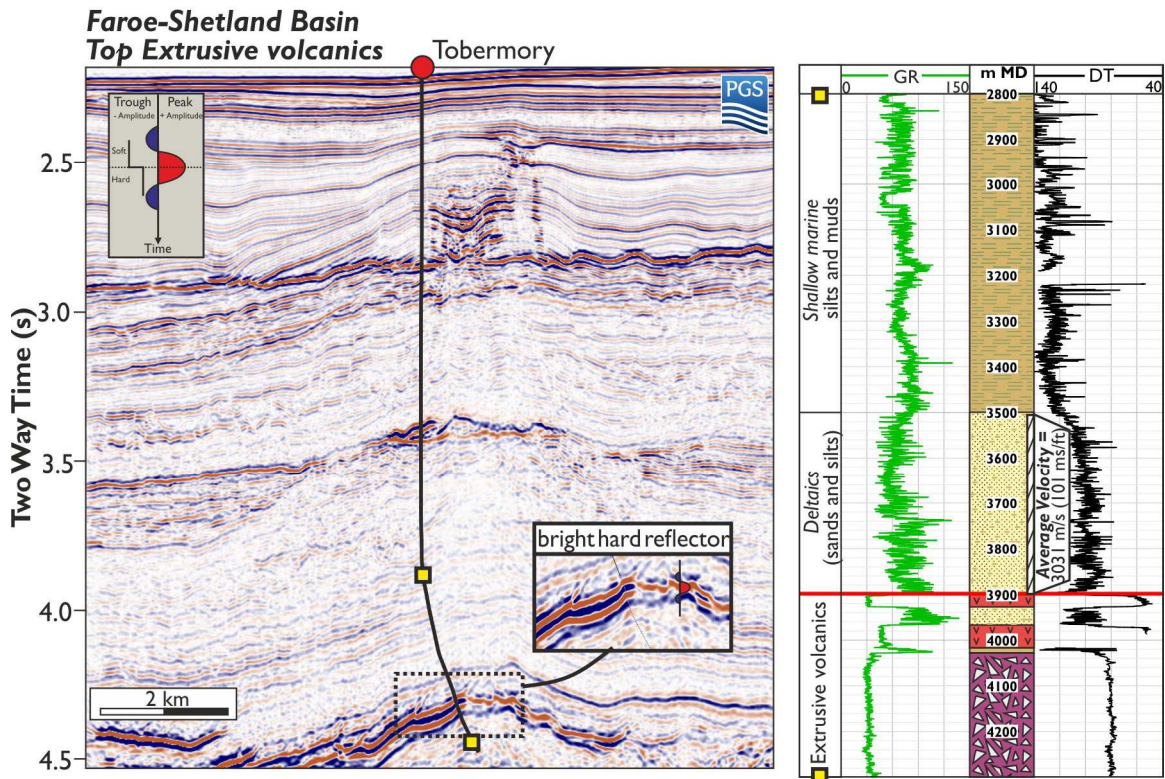
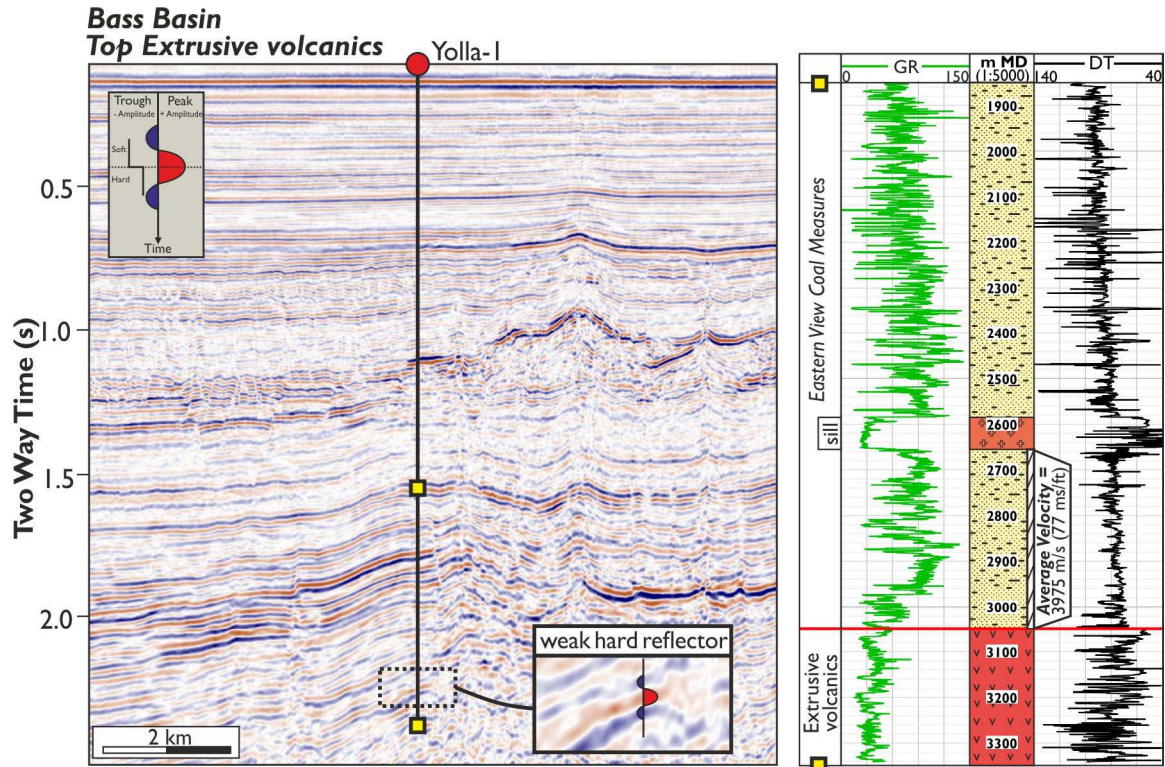


AC





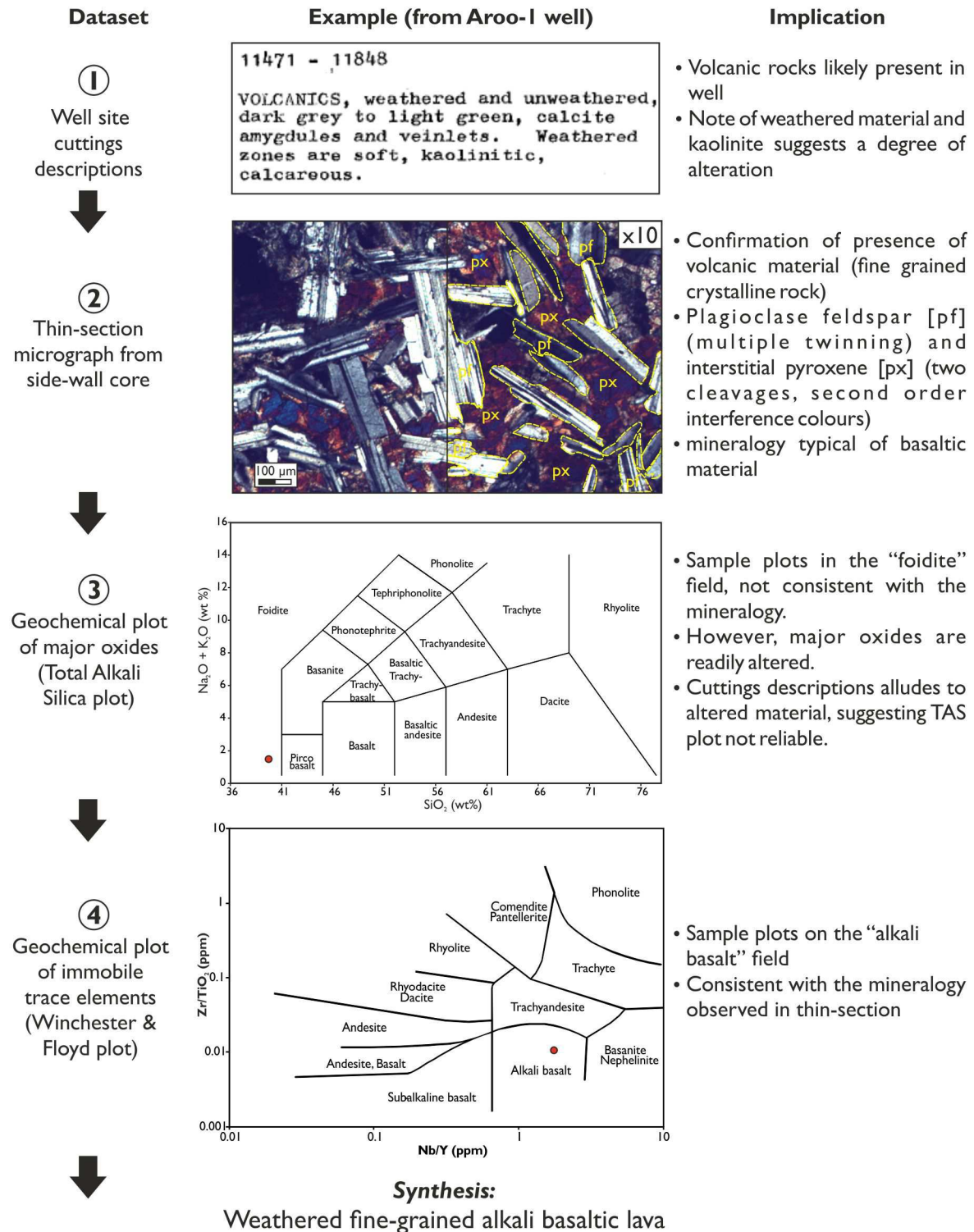




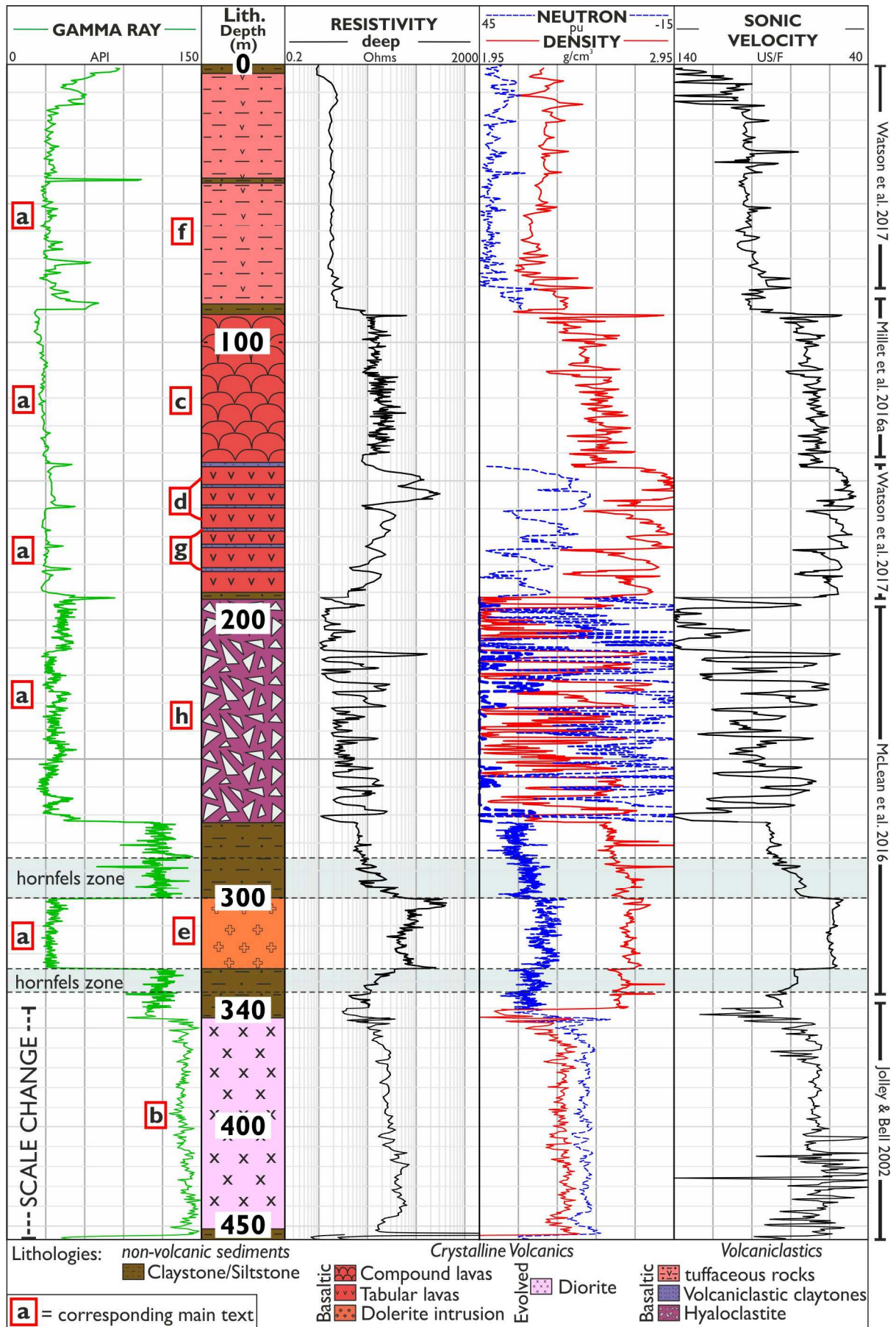


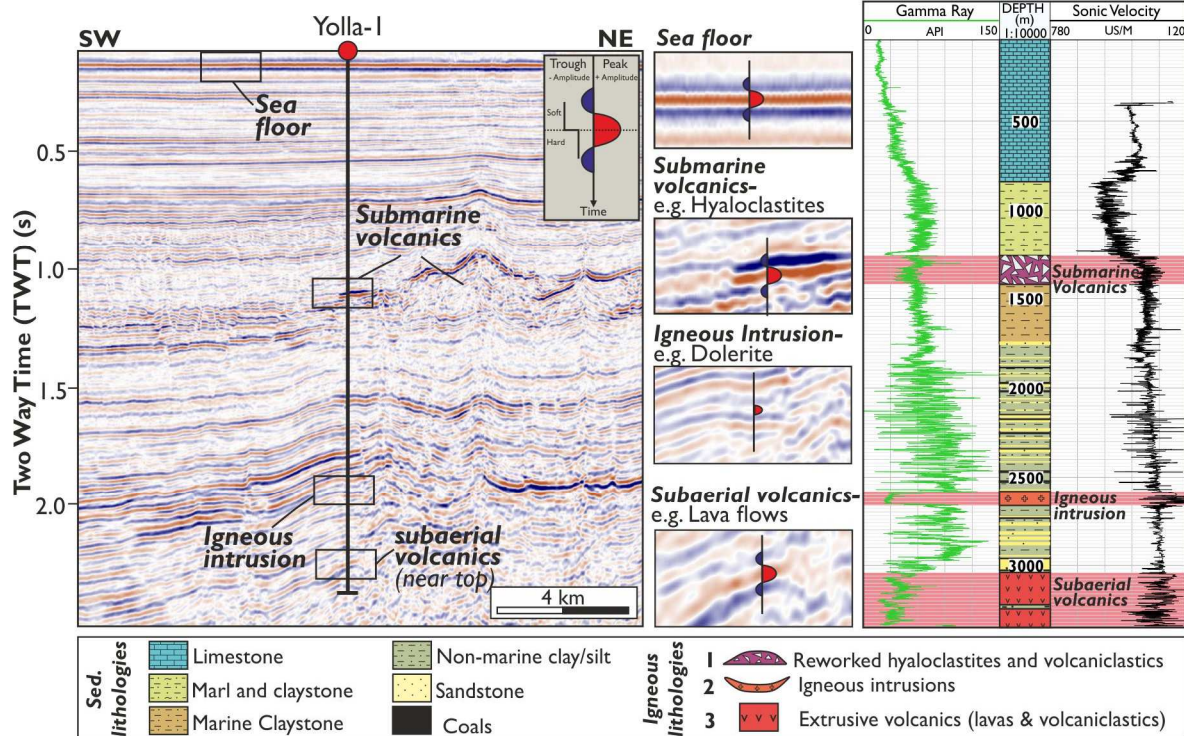
Age Ma BP	Era	Epoch	Stage	Spore- Pollen Zone	Seq.	Litho- Strat.		
10	CENOZOIC	O	Calabrian	<i>T. pleistocenicus</i>	TORQUAY	TORQUAY		
			Piacenzian	<i>M. lipsis</i>				
			Zanclean	<i>C. bifurcatus</i>				
		L	Messinian					
			Tortonian					
			Serravillian	<i>T. bellus</i>				
		M	Langhian					
			Burdigalian					
			Aquitanian					
		E	OLIG	Chattian			<i>P. tuberculatus</i>	
				Rupelian				
				Priabonian				
		L	EOCENE	Bartonian			<i>N. Asperus</i>	
				Lutetian				
				Ypresian			<i>P. asperopolus</i>	
E	PAL	Thanetian						
		Selandian	<i>L. balmei</i>					
		Danian						
70	MESOZOIC	CRETACEOUS	LATE	Maastrichtian	<i>F. longus</i>	EASTERN VIEW COAL MEASURES		
					<i>T. lillei</i>			
				Campanian	<i>N. senectus</i>			
			Santonian	<i>T. apoxyxinus</i>	DURROON		LOWER DURROON Fm.	
				Coniacian				<i>P. mawsonii</i>
				Turonian				<i>H. uniforma</i>
			Cenomanian	<i>P. pannosus</i>	OTWAY		OTWAY GROUP	
				Albian				<i>C. paradoxa</i>
								<i>C. striatus</i>
			Aptian	<i>P. notensis</i>	CRAYFISH		CRAYFISH GROUP (equivalent)	
				Barremian				<i>F. wonthaggiensis</i>
				Hauterivian				
			Valanginian					
				Berriasian	<i>C. australiensis</i>			
			140	CENOZOIC	O		Calabrian	<i>T. pleistocenicus</i>
Piacenzian	<i>M. lipsis</i>							
Zanclean	<i>C. bifurcatus</i>							
L	Messinian							
	Tortonian							
	Serravillian	<i>T. bellus</i>						
M	Langhian							
	Burdigalian							
	Aquitanian							
E	OLIG	Chattian			<i>P. tuberculatus</i>			
		Rupelian						
		Priabonian						
L	EOCENE	Bartonian			<i>N. Asperus</i>			
		Lutetian						
		Ypresian			<i>P. asperopolus</i>			
E	PAL	Thanetian						
		Selandian	<i>L. balmei</i>					
		Danian						
70	MESOZOIC	CRETACEOUS	LATE	Maastrichtian	<i>F. longus</i>	EASTERN VIEW COAL MEASURES		
					<i>T. lillei</i>			
				Campanian	<i>N. senectus</i>			
			Santonian	<i>T. apoxyxinus</i>	DURROON		LOWER DURROON Fm.	
				Coniacian				<i>P. mawsonii</i>
				Turonian				<i>H. uniforma</i>
			Cenomanian	<i>P. pannosus</i>	OTWAY		OTWAY GROUP	
				Albian				<i>C. paradoxa</i>
								<i>C. striatus</i>
			Aptian	<i>P. notensis</i>	CRAYFISH		CRAYFISH GROUP (equivalent)	
				Barremian				<i>F. wonthaggiensis</i>
				Hauterivian				
			Valanginian					
				Berriasian	<i>C. australiensis</i>			

## Workflow for investigating volcanic rocks at a micro-scale

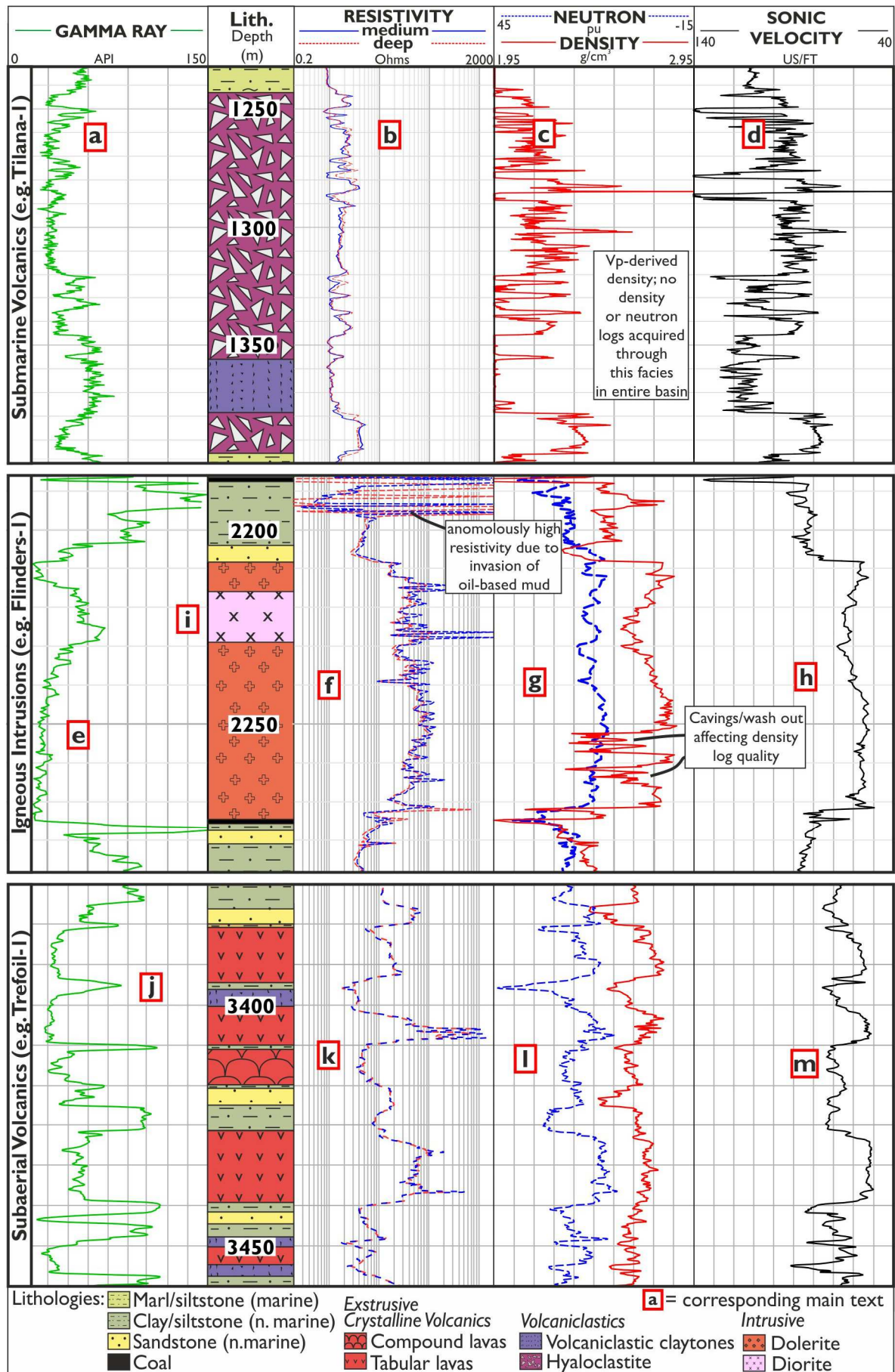


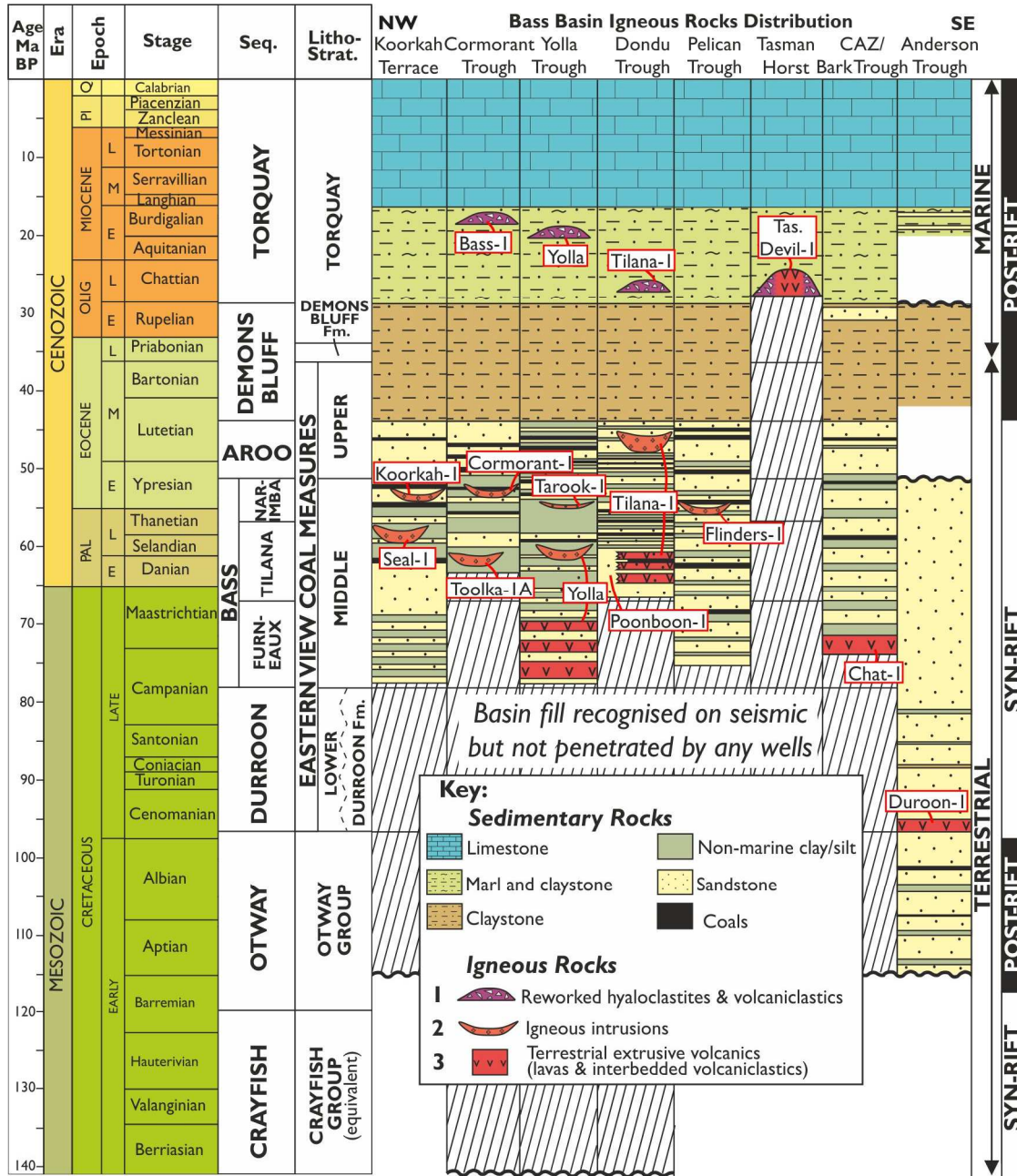


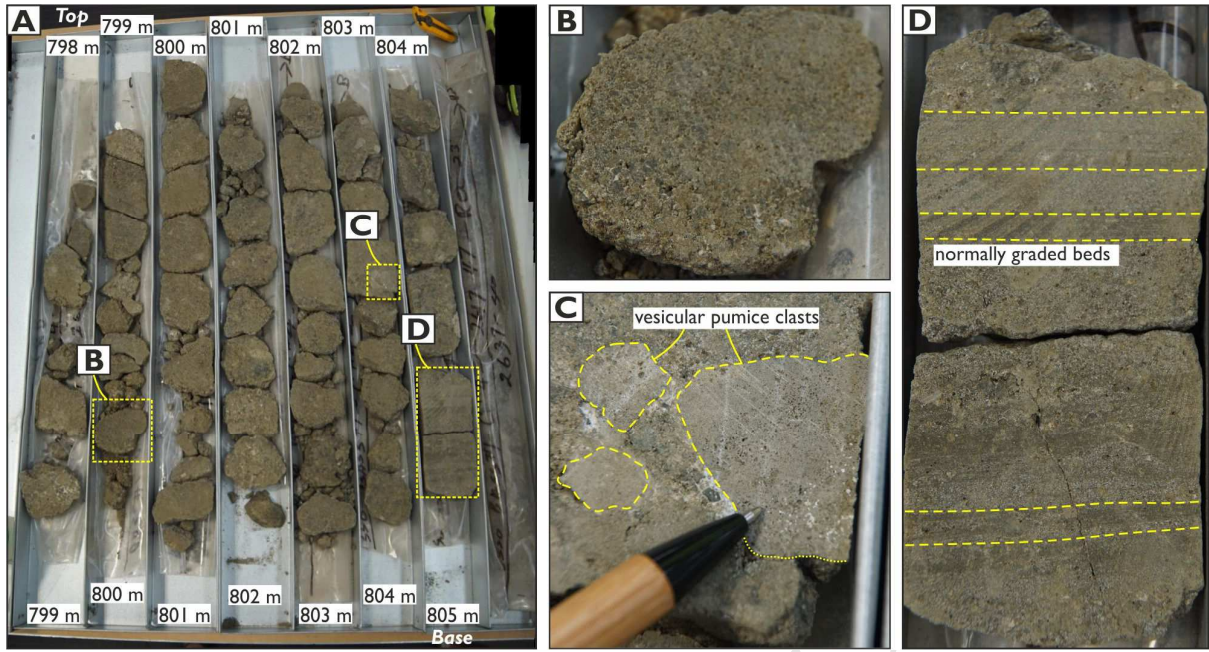




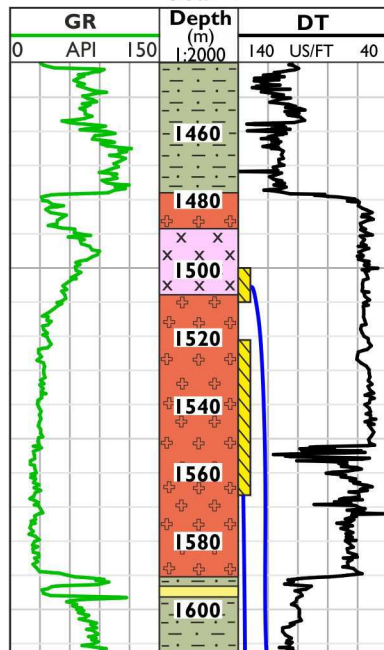
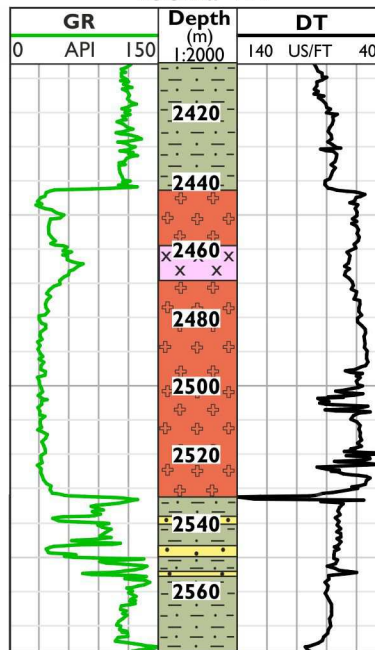
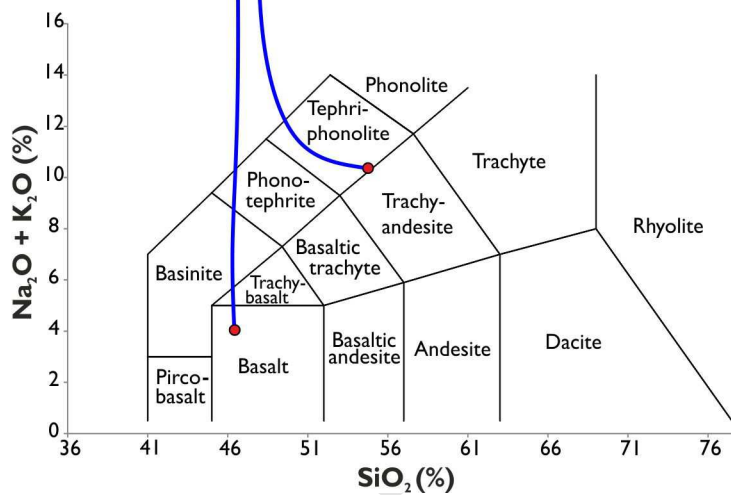
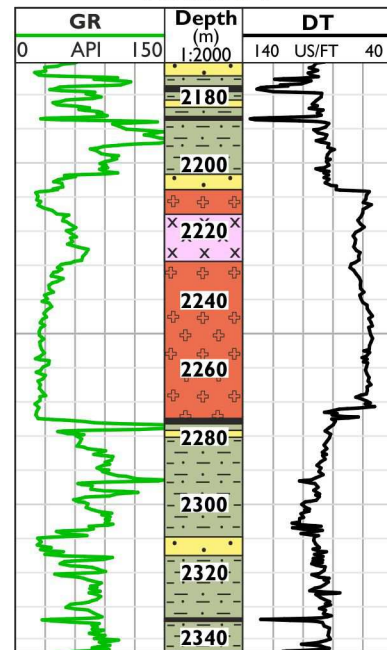










NW Koorkah Terrace  
Seal-ICormorant Trough  
Toolka-1APelican Trough SE  
Flinders-1

## Key:

## Sedimentary rocks

Clay/siltstone (n. marine)

Sandstone (n.marine)

Coal

## Igneous intrusions

Dolerite

Silicic intrusion

Interval where geochemistry was obtained from cuttings

- The Bass Basin is a Mesozoic-Cenozoic intra-continental rift basin along southern Australian
- Igneous rocks encountered in 20 out of 36 (55.6%) exploration wells drilled within the Bass Basin
- In 13 of 20 exploration wells (65%) the igneous rocks encountered were not predicted pre-drill
- Anomalously low acoustic impedance contrast between igneous rocks and sedimentary sequences in the Bass Basin, relative to other basins notable for magmatism, such as the North Atlantic Margin.